AD-A169 678 IDENTIFICATION OF DAMPING PARAMETERS OF A SQUEEZE-FILM BEARING(U) SUSSEX UNIV BRIGHTON (ENGLAND) J B ROBERTS MAY 86 DAJA45-84-C-0044 1/1

UNCLASSIFIED F/G 20/11 NL

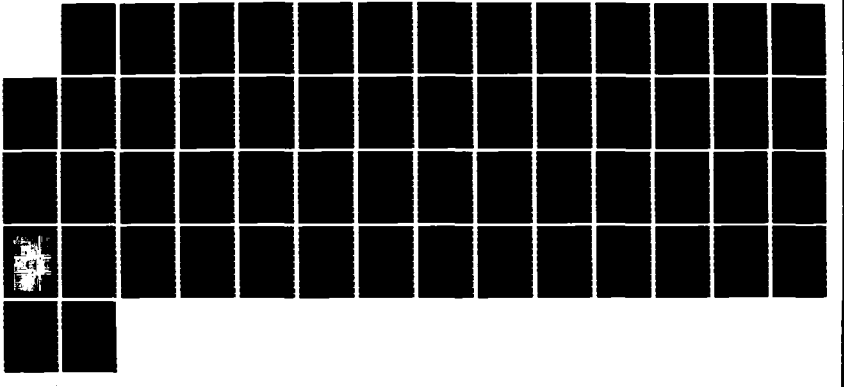

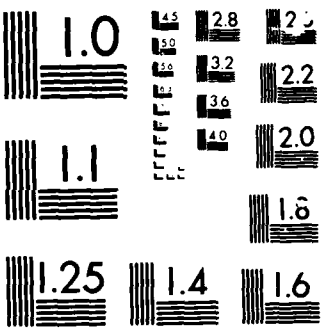
1.0
1.1
1.25
1.4
1.6
2.8
3.2
3.6
4.0
2.2
2.0
1.8

R&D 4005A-AN

REPORT DOCUMENTATION PAGE

READ INSTRUCTIONS BEFORE COMPLETING FORM

1. REPORT NUMBER	2. GOVT ACCESSION NO.	3. RECIPIENT'S CATALOG NUMBER

4. TITLE (and Subtitle)
Identification of Damping Parameters of a Squeeze-Film Bearing

5. TYPE OF REPORT & PERIOD COVERED
Final Technical Report
Oct 84 - Oct 85

6. PERFORMING ORG. REPORT NUMBER

7. AUTHOR(s)
Dr. J.B. Roberts

8. CONTRACT OR GRANT NUMBER(s)
DAJA45-84-C-0044

9. PERFORMING ORGANIZATION NAME AND ADDRESS
University of Sussex
U.K.

10. PROGRAM ELEMENT, PROJECT, TASK AREA & WORK UNIT NUMBERS
61102A
1L161102BH57-06

11. CONTROLLING OFFICE NAME AND ADDRESS
USARDSG-UK
Box 65, FPO NY 09510-1500

12. REPORT DATE
May 1986

13. NUMBER OF PAGES
46

14. MONITORING AGENCY NAME & ADDRESS (if different from Controlling Office)

15. SECURITY CLASS. (of this report)
Unclassified

15a. DECLASSIFICATION/DOWNGRADING SCHEDULE

16. DISTRIBUTION STATEMENT (of this Report)
Approved for Public Release; distribution unlimited

17. DISTRIBUTION STATEMENT (of the abstract entered in Block 20, if different from Report)

18. SUPPLEMENTARY NOTES

19. KEY WORDS (Continue on reverse side if necessary and identify by block number)
Vibration Control; Squeeze-film bearings; Damping measurements; Parametric identification; Inertial effects

20. ABSTRACT (Continue on reverse side if necessary and identify by block number)
This report describes the results obtained from a combined experimental and theoretical programme concerned with the determination of the damping and inertial coefficients of a squeeze-film bearing, and the dependence of these coefficients on eccenticity ratio and frequency of vibration.
The experimental results were obtained from a new experimental rig, in which the squeeze-film journal is mounted on a beam of continuously variable length.

20. Contd.

By means of a transient test technique, combined with signal processing, based on a parametric identification method, estimates of the damping and inertial coefficients have been obtained for static eccentricity ratios in the range 0.0 to 0.5, and for frequencies of vibration ranging from 50 Hz to 180 Hz. These coefficients are, in general, much higher in value than the conventional short-bearing theory for squeeze-film bearings predicts (by a factor of 10, in some cases) suggesting serious inadequacies in the available theoretical prediction procedures.

In an attempt to explore possible theoretical deficiencies, with respect to the evaluation of inertial coefficients, numerical theoretical predictions of these coefficients were obtained for finite-length bearings, with various L/D ratios (where L is the length of one bearing land, and D is the diameter of the bearing). The technique used, based on a finite difference solution of a two-dimensional partial differential equation for the "inertial pressure" distribution, was found to give good agreement with some other theoretical results, obtained by much more complex methods. However, the effect of the finite width of the bearing was found to be weak, for the squeeze-film geometry of interest here - i.e., the short-bearing theory was found to be an adequate approximation. Thus, this theoretical investigation has not revealed the basic source of discrepancy between the measured coefficients and the short-bearing theory, based on conventional assumptions regarding the fluid flow.

This report describes the experimental and theoretical aspects of the present investigation in two parts, referred to as part one and two, respectively, followed by some concluding remarks on the investigation as a whole.

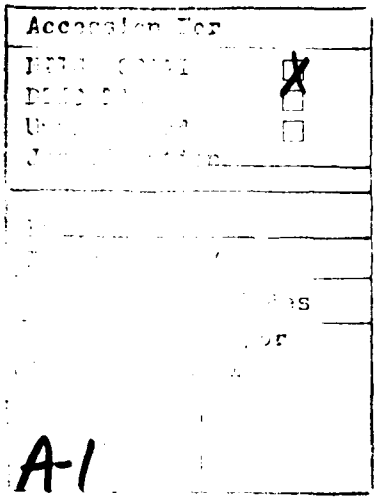

IDENTIFICATION OF DAMPING PARAMETERS OF A SQUEEZE-FILM BEARING

Final Technical Report

by

Dr. J.B. Roberts

May 1986

United States Army
EUROPEAN RESEARCH OFFICE OF THE U.S. ARMY
London, England.

CONTRACT NUMBER DAJA45-84-C-0044

University of Sussex,

Summary

This report describes the results obtained from a combined experimental and theoretical programme concerned with the determination of the damping and inertial coefficients of a squeeze-film bearing, and the dependence of these coefficients on eccentricity ratio and frequency of vibration.

The experimental results were obtained from a new experimental rig, in which the squeeze-film journal is mounted on a beam of continuously variable length. By means of a transient test technique, combined with signal processing based on a parametric identification method, estimates of the damping and inertial coefficeints have been obtained for static eccentricity ratios in the range 0.0 to 0.5, and for frequencies of vibration ranging from 50 Hz to 180 Hz. These coefficients are, in general, much higher in value than the conventional short-bearing theory for squeeze-film bearings predicts (by a factor of 10, in some cases) suggesting serious inadequacies in the available theoretical prediction procedures.

In an attempt to explore possible theoretical deficiencies, with respect to the evaluation of inertial coefficients, numerical theoretical predictions of these coefficients were obtained for finite-length bearings, with various L/D ratios (where L is the length of one bearing land, and D is the diameter of the bearing). The technique used, based on a finite difference solution of a two-dimensional partial differential equation for the "inertial pressure" distribution, was found to give good agreement with some other theoretical results, obtained by much more complex methods. However, the effect of the finite width of the bearing was found to be weak, for the squeeze-film geometry of interest here - i.e., the short-bearing theory was found to be an adequate approximation. Thus, this theoretical investigation has not revealed the basic source of discrepancy between the measured coefficients and the short-bearing theory, based on conventional assumptions regarding the fluid flow.

This report describes the experimental and theoretical aspects of the present investigation in two parts, referred to as part one and two, respectively, followed by some concluding remarks on the investigation as a whole.

List of Keywords

Vibration control
Squeeze-film bearings
Damping measurements
Parametric identification
Inertial effects

CONTENTS

List of Illustrations

List of Tables

PART ONE

PART ONE: EXPERIMENTAL INVESTIGATIONS

NOTATION

A	true non-dimensional start displacement for free-decay data
b_{rr}, b_{ss}	direct fluid damping coefficients, for the r and s directions, respectively
B_{rr}, B_{ss}	non-dimensional direct fluid film damping coefficients, for the r and s directions, respectively
c	radial clearance between journal and bearing
c_{rr}, c_{ss}	direct fluid film inertial coefficients, for the r and s directions, respectively.
d	initial displacement
d^*	non-dimensional initial displacement ($= d/c$)
e	mean square error between fitted theoretical decay curve and experimental data
k_r, k_s	beam stiffness, in the r and s directions, respectively
ℓ	land length of bearing
m	effective first mode mechanical mass
m_H	hydrodynamic mass (c_{rr} in radial direction, c_{ss} in transverse direction)
r	journal displacement in the radial direction (i.e in the direction of the attitude line)
R	radius of the journal
Re	Reynolds number ($= \rho\omega c^2/\eta$)
s	journal displacement in the transverse direction (i.e. in a direction perpendicular to the attitude line)
t	time
t_G	guessed start time
t_T	true start time
$X(t)$	non-dimensional displacement
X_i	measured, free-decay record
X^*_i	analytical solution to equation (4)
U	objective function, defined by equation (11)

γ^*	non-dimensional damping parameter
γ_o^*	value of γ^*, in the absence of the fluid film
δ^*	non-dimensional stiffness parameter
δ_o^*	value of δ^*, in the absence of the fluid film
ϵ	eccentricity ratio
ϵ_o	static eccentricity ratio
λ	parameter defined by equation (10)
η	absolute viscosity of the squeeze-film fluid
ρ	density of the squeeze-film fluid
Δt	sampling interval
δt	difference between t_G and t_T
ω	frequency of vibration
ω_o	natural frequency of undamped vibration ($\omega = \omega_{ro}$, for radial motion, and $\omega = \omega_{so}$, for transverse motion)
τ	non-dimensional time

SUMMARY

A technique for obtaining estimates of the direct damping and inertial coefficients of a squeeze-film bearing is described. This involves applying parametric identification and optimisation techniques to digitised, free-decay experimental displacement records. The experimentally obtained coefficients, derived by this technique, were found to be significantly higher in magnitude (in some cases by a factor of about 10) than the corresponding values derived from conventional short-bearing theory, and to be virtually independent of the frequency of vibration.

1. INTRODUCTION

The squeeze-film damper has proved a useful means of eliminating instabilities and reducing vibration in rotor-bearing systems, such as occur, for example, in aero-engines (e.g. see Refs 1 and 2).

For squeeze-film dampers with a centralising spring it is possible to model their dynamic behaviour in terms of damping coefficients, which can be estimated theoretically from a solution of Reynolds equation (e.g. see Ref.3). Recently it has been demonstrated theoretically, by a number of workers [4-10], that inertial effects within the lubricant can also be significant and that the normal damping coefficient representation should be augmented to include acceleration, or inertial coefficients. In many applications these latter coefficients are important since the gap Reynolds number

$$Re = \frac{\rho\omega c^2}{\eta} = \frac{\text{fluid inertia force}}{\text{fluid viscous force}}$$

is of order one, or greater; here ρ is the density of the lubricant, ω is the frequency of vibration, c is the radial clearance of the squeeze-film damper and η is the absolute viscosity of the lubricant.

Despite these advances in theoretical understanding there has been a distinct lack of supporting experimental measurements, particularly with regard to the effect of fluid inertia, and agreement between theory and available experimental results is generally rather inconclusive (e.g. see Refs. 11-14). In an effort to improve this situation a recent experimental investigation was carried out, using parametric identification techniques, for the purposes of obtaining estimates of damping and inertial coefficients from transient test data [15]. The results, which covered the Reynolds number range $0.5 < Re < 1.5$, indicated that the inertial effect was significantly greater than that predicted by available theories.

The objective of the present paper is to present some new experimental measurements of damping and inertial coefficients. The same basic test procedure as described in reference [15] was employed but the data was obtained from an entirely new rig, which allowed a continuous variation of the

frequency of vibration. Moreover, the squeeze-film geometry used in the present investigation was closer to that used in typical aero-engine applications. The results relate to a higher frequency range (50Hz to 180Hz) than that in [15]; the corresponding Reynolds number range is $1.05 < Re < 3.64$.

2 THE EQUATIONS OF MOTION

For a squeeze-film damper with a centralising spring, small motion of the journal, with respect to a fixed bearing, can be described by a pair of second order equations of motion. These equations are conveniently written in terms of the radial, r, and transverse, s, displacements, where these are measured from the static eccentricity position. For free motion, in the radial direction only, the equation of motion for r is simply

$$(m+c_{rr})\ddot{r} + (b_f^Q + b_{rr})\dot{r} + k_r r = 0 \qquad (1)$$

where c_{rr} is a radial inertial (or acceleration) coefficient and b_{rr} is a radial damping coefficient for the squeeze-film, b_f^Q denotes structural damping and k_r is the stiffness of the centralising spring; m is the mass of the squeeze-film journal. For free motion in the transverse, s, direction an equation of motion similar to equation (1) applies; the relevant squeeze-film coefficients are now c_{ss}, the transverse inertial coefficient and b_{ss}, the transverse damping coefficient.

Both these equations of motion for free vibration can be written in a standard form. As a first step it is convenient to non-dimensionalise by introducing the non-dimensional time variable

$$\tau = \omega_o t \qquad (2)$$

where ω_o is the frequency of undamped vibration ($\omega_o = \omega_{or}$, for radial motion), and $\omega_o = \omega_{os}$, for transverse motion, and the non-dimensional displacement

$$X(t) = \frac{\text{displacement (at t)}}{\text{initial displacement (at t=0)}} \qquad (3)$$

The standard form is then

$$\ddot{X} + \gamma^* \dot{X} + \varepsilon^* X = 0 \qquad (4)$$

where γ^* is a non-dimensional damping coefficient and ε^* is a non-dimensional stiffness coefficient.

Through a comparison of equations (1) and (4) one readily finds that, for the radial motion,

$$b_{rr} = m\,\omega_{ro}\left[\frac{\gamma^*}{\varepsilon^*} - \gamma_o^*\right] \qquad (5)$$

and

$$c_{rr} = m\left[\frac{1}{\varepsilon^*} - 1\right] \qquad (6)$$

where γ_o^* is the value of γ^* in the case of no fluid film in the squeeze-film damper - i.e. the structural damping component of γ^*. Similar equations for b_{ss} and c_{ss} can be written.

Equations (5) and (6) provide a simple means of determining b_{rr} and c_{rr} (and also, of course, b_{ss} and c_{ss}) from free-decay tests. Thus, for example, from a measured free-decay in the radial direction only, values of γ^* and δ^* may be found by fitting equation (4), in some sense, to the experimental data. Similarly, γ_o^* and ω_{ro} may be determined from a free-decay test without lubricant in the damper. Equations (5) and (6) can then be applied to yield estimates of b_{rr} and c_{rr}.

In the tests to be described later the centralising spring was realised by mounting the squeeze-film journal centrally on a beam, built-in at both ends. Free-decay motion was obtained by applying a force to the centre of the journal, to give the journal an initial displacement, and then releasing the force. For such a system many modes of vibration can, in principle, exist simultaneously; however, it is easy to show that the first mode will be entirely dominant and thus that an equation of motion of the form of equation (4) is appropriate. In these circumstances the mass m appearing in equations (5) and (6) can be interpreted as the effective, first mode mass. It can be determined very easily by a direct measurement of the beam stiffness, k, and the undamped natural frequency of vibration, ω_o.

For the case of a short full-film squeeze-film damper, which is of interest here, theoretical expressions of b_{rr} and b_{ss} have been known for some time [16]. Corresponding theoretical results for c_{rr} and c_{ss} have been given by Smith [17]. These results are collected together in Table 1. It has been shown recently by the authors [18] that Smith's theoretical results are in very close agreement with the results of the more elaborate analyses given by Reinhardt and Lund [8] and Szeri et al [9]

It is noted that these theoretical results are strictly valid for small values of Re (Re << 1), whereas in the present experiments Re > 1. However, theoretical investigations into the influence of finite Reynolds number on the force coefficients (e.g. see Refs 19 and 20) suggest that, for the squeeze-film geometry of concern here, this influence is likely to be small.

3. EXPERIMENTAL FACILITY AND PROCEDURE

3.1 Experimental rig

The experimental rig is shown by a photograph in Fig.1(a) and as a line diagram in Fig. 1(b). The journal of the squeeze-film damper was non-rotating but free to vibrate, as a result of external disturbances, in any direction orthogonal to its axis. It was contained within a circular bearing and supported by a beam of circular cross-section. This beam, which provided a stiffness in parallel with the squeeze-film

(i.e. acted as a centralising spring) was clamped rigidly, through a collet connection, to support brackets, positioned symmetrically on each side of the journal. The effective length of the support beam could be varied, fairly easily, by varying the position of the support clamps. In this way it was possible to vary the effective spring stiffness of the beam, and hence the natural frequency of the first mode of vibration, over a fairly wide range. In addition to this adjustment, screw actuated positioning devices allowed the bearing to be moved independently in both the horizontal and vertical directions (perpendicular to the beam axis); thus any desired static eccentricity position, of the journal relative to the bearing, could be readily achieved. Accurate static positioning was obtained by outputting displacement transducer signals to the computer display screen whilst the operating screws were adjusted.

The bearing consisted of two plain lands separated by a central circumferential groove. Lubricant (in this case Tellus R10) was supplied to the groove by a pump through three 2BA, 3/4" deep holes, spaced 120^{o} apart around the bearing. No end seals were employed, so the lubricant simply discharged freely into a reservoir before being recirculated. The relevant bearing dimensions were as follows:

Bearing land length	9.0mm
Journal radius	68.0mm
Radial clearance	0.22mm
Central groove width	4.0mm
Central groove depth	0.5mm

3.2 Experimental procedure and data acquisition

In the experimental work, tests were carried out for natural frequencies of vibration of 50Hz, 80Hz, 128Hz, 150Hz and 180Hz (it is noted that the differences between ω_{ro} and ω_{so} were found to be very small in practice; this distinction will, therefore, not be made in future discussion). In each case the effective spring stiffness of the beam was determined experimentally by simply pulling the journal horizontally, with a known static force, and measuring the resulting journal displacement. From this information, and the measured natural frequencies, it was possible to determine the effective journal mass, m, at each natural frequency.

For each of the natural frequencies chosen, a series of test was conducted, at various values of static eccentricity ratio. In each test the journal was pulled through an "initial displacement" to an "initial position" within the clearance circle, by a length of wire looped over a pin attached to the core of a solenoid. The journal was then released by actuating the solenoid; this had the effect of rapidly retracting the pin and hence freeing the wire. The subsequent transient, decaying oscillatory motion of the journal was measured by proximity capacitive probes clamped adjacent to datum surfaces on the vibrating journal and recorded by computer.

In the present series of tests the static eccentricity

position was always on the vertical radial line and radial and transverse free decays were measured separately by pulling the journal in the vertical and horizontal directions, respectively. For each static eccentricity value results were obtained for (a) the journal centre the required distance above the bearing centre and (b) the journal centre the same distance below the bearing centre, and the results finally averaged.

For each transient test it was possible to measure, simultaneously, both horizontal and vertical motions. It was observed experimentally that, as one would expect from the theory, a perturbation of the journal in one direction (either radial or transverse) did not result in any significant motion in the perpendicular direction. In fact, motion in the perpendicular direction was found to be less than one per cent of the amplitude of the motion in the direction of initial displacement. Thus, in the main body of the experimental work, only the motion in the direction of the initial displacement was measured and recorded.

Throughout the tests the supply pressure of the lubricant was maintained at 14 kN/m^2, to ensure that full-film lubrication conditions pertained in the squeeze-film. The temperature of the lubricant was measured at the outlet of the bearing and recorded for each test. The corresponding lubricant viscosity was then obtained from a calibration curve. The viscosity changed significantly with temperature. Thus at 20^oC, $\eta = 0.0188$ Ns/m^2, whereas at 30^oC, $\eta = 0.0122$ Ns/m^2.

To avoid the necessity of processing and graph plotting the decay data manually, a microprocessor based, purpose-built data acquisition system was developed for use in this work; this could also be used for initiating a test. An initiation pulse, generated by the microprocessor was used to activate a relay and hence energise the solenoid and release the journal; this pulse also simultaneously started analogue to digital conversion (ADC) of the journal displacement signal coming from the rig. The sampling interval, Δt, in the ADC conversion could be varied, under software control. The equi-spaced samples of the free-decay were stored, and then transmitted to a main-frame computer, for subsequent processing.

4 ESTIMATION OF PARAMETERS

As explained in the preceding section, the proposed procedure requires the estimation of γ^* and ε^*, in equation (4), from normalised, experimental free-decay data. The data was in the form of n equi-spaced digital samples, X_i, ($i = 0,1,\ldots,n-1$). The estimation technique employed here is a combination of a parametric identification method (previously used in ref [15]) and an optimisation method.

4.1 Parametric identification

In ref [15] an iterative algorithm for identifying the parameters γ^* and ε^* in equation (4) was developed, based on the sequential least-square method of Detchmendy and Stridhar [21]. This method, also used in the present work, generates

sequential estimates of the state variables X(t) and $\dot{X}$(t) and also estimates of γ^* and ζ^*, at the times $i\Delta t$. These estimates "track" the experimental data and generally converge to stable values as time increases. By applying the method iteratively, improved estimates of γ^* and ζ^* can be found. Thus, in the first iteration, γ^* and ζ^* are guessed, and these values are used to start the sequential estimation computation. The estimates obtained at the end of the data sequence are then used, in place of the initial guess, to start the next iteration. By repeating the iteration a number of times, the estimates of γ^* and ζ^*, at the end of the data sequence, are found to converge to constant values.

4.2 Optimisation method

A difficulty with the method just described is that the exact time of release, i.e. the true start time of the free decay, is not known accurately. This is because there is a finite time required to energise the solenoid and retract its pin. This delay time was found to vary somewhat from test to test, due to the use of an AC supply voltage to energise the solenoid. The ADC conversion invariably starts before the time of release and hence one could, from a visual inspection of the data samples, estimate the true start time, to the nearest sampling instant. However, the error in this estimation, which depends on the sampling interval, can significantly influence the values of the estimates of γ^* and ζ^*.

This difficulty was overcome here by fitting the exact analytical solution for equation (4) to the experimental data, using an optimisation technique. The approach is illustrated by Fig.2. If t_G is the guessed start time, and t_T is the true start time then there are two cases: (a) $t_G < t_T$ (shown in Fig.2(a)) and (b) $t_G > t_T$ (shown in Fig.2(b)). In both cases, in addition to the unknown parameters γ^* and ζ^*, there are the unknown variables $\delta t = t_T - t_G$ and A, the true start amplitude. It is therefore required to minimise the difference between the analytical solution of equation (4) and the set of experimental values, X_i, $i = 0,1,\ldots,n-1$, by optimising the values of δt, A, γ^* and ζ^*.This is achieved through a least-squares fit of the analytical solution to the experimental data.

Thus, if

$$t_i = i\Delta t - \delta t \qquad (i = 0,1,\ldots,n-1) \qquad (7)$$

then the analytical solution is

$$X_i^* = A \qquad \text{for } t_i \leq 0 \qquad (8)$$

and, for damping less than critical,

$$X_i^* = A e^{-\frac{\gamma^* t_i}{2}} \left[\sin\left(\frac{\gamma^* \lambda t_i}{2}\right) + \lambda \cos\left(\frac{\gamma^* \lambda t_i}{2}\right)\right] \qquad \text{for } t_i > 0 \qquad (9)$$

where

$$\lambda = \left(\frac{4\delta^*}{\gamma^{*2}} - 1\right)^{1/2} \qquad (10)$$

Similar expressions for X_i^* can be written for damping equal to, or greater than, critical.

A least-squares fit is achieved by minimising the objective function

$$U = \sum_{i=0}^{n=1} (X_i - X_i^*)^2 \qquad (11)$$

where the ranges of the parameters γ^* and δ^* are unrestricted. The particular optimisation algorithm adopted here is a variant of the PATSH, a direct search strategy developed by Whitney, and presented by Johnson [22]. In this version a progressively centred "shot-gun" or random search is made at the end of each direct search stage in an attempt to avoid "hang-ups" at non-optimal points. In the present application the four-dimensional optimisation search procedure is very much simplified due to the absence of problem constraints.

Clearly the speed of convergence of the optimisation method depends on the accuracy of the initial parameter estimates. Here the parametric identification method, described in the previous section, was used to generate the initial estimates of γ^* and δ^*, whilst the initial estimates of δt and A were taken to be 0 and 1 respectively. With these start values the optimisation method was found to be very rapid and efficient.

5 EXPERIMENTAL RESULTS

For each test condition (i.e. each prescribed value of ϵ_o and ω_o, and each specified direction of motion) several (typically five to seven) individual free-decay records were obtained. Fig.3(a) shows five such individual data records for a typical case (ϵ_o = 0.2, ω_o = 80Hz, radial motion), with a sampling interval of 0.25ms. Here the equi-spaced samples have been linearly interpolated. The variations in the data, within this set, are due to (a) electronic noise in the displacement measuring system, (b) analogue to digital quantisation noise (here 8 bit resolution was employed) and (c) uncertainty in the true start time, as discussed earlier. However, it is clear that, given the above factors, very good repeatability of free-decay data was obtained. The effect of noise could be substantially reduced by averaging the set of results at each test condition; thus, for example, the effect of averaging the data shown in Fig.3(a) is shown as the much smoother decay curve in Fig.3(b).

After averaging, at each test condition, the data were processed using the techniques described briefly in section 4. Fig.4 shows some typical comparisons between the fitted theoretical curves and the averaged experimental data, for the case where ϵ_o = 0, ω_o = 180Hz and the direction of motion was radial. For data acquired at the relatively large sampling interval of 0.5ms, as shown in Fig.4(a), it is evident that the parametric identification technique of Ref.[21] results in

a rather poor fit to the experimental data (note that here the theoretical curve is the exact solution to equation (4), computed using the estimated values of γ^* and ζ^*). This discrepancy arises directly from the use of a relatively large sampling interval, which leads to (a) significant truncation errors in the finite difference approximation to the basic differential algorithm of Ref.[21] and (b) a significant error due to the uncertainty in the start time. However, when the optimisation technique, based on the exact analytical solution, was employed as a second stage in the analysis, then a much improved fit to the experimental data was obtained, as shown in Fig.4(a). It can be expected, therefore, that the parameter estimates obtained from the optimisation procedure are significantly more accurate than the original, "identified parameters", derived by the method of Ref.[21].

As the sampling interval is reduced one can expect that the identification method will improve in accuracy and that the refinement in estimation obtained through the optimisation method will be less significant. This was indeed found to be the case, as is shown, for example, by the results in Fig.4(b); here, for the same test conditions as in Fig.4(a), a sampling rate of 0.25ms was used to acquire the data. At this higher sampling rate it is evident that the improvement in fit, through the second level of analysis, based on optimisation, is much less significant.

Table 2 shows the value of the total mean square error, e, between the fitted theoretical decay curves and the experimental data (for the optimisation method e = U/n, where U is the objective function defined by equation (11)); this corresponds to the results shown graphically in Fig.4. Clearly, for Δt = 0.5ms the value of e has been reduced by up to 50%, by means of the optimisation technique, whereas at Δt = 0.25ms the maximum improvement obtained, over the identification technique, is about 12%.

In the light of these, and other similar results, it was decided to process all the averaged decay curves using the combined identification-plus-optimisation method - i.e. using the identification procedure to provide the initial guesses of γ^* and ζ^* for the optimisation calculation. It is noted, however, that strictly this analysis method should be applied to the individual free-decay data, prior to averaging, and that the estimated parameters from each individual data record should subsequently be averaged to produce final estimates of γ^* and ζ^*. However, experience showed that the values of γ^* and ζ^* derived from the individual records, when averaged, were very close to the values deduced directly from the averaged data. Some typical estimates for γ^* and ζ^* are shown in Table 3, for the case of ϵ_o = 0.2, ω_o = 80Hz, and radial motion (see Fig.3 for the corresponding experimental data). It is seen from the results in this table that the estimates derived from individual tests (see Fig.3(a)) show a low variability and that their averaged values, γ^* = 0.553 and ζ^* = 0.898, are very close to the corresponding values, γ^* = 0.549 and ζ^* = 0.907, derived by analysing the averaged data (see Fig.3(b)). All the results presented subsequently here were accordingly derived by processing the averaged data, at each test condition, since this involved much less

computation effort than the processing of individual data records.

Figs.5(a) to (d) show some typical comparisons between averaged experimental data and fitted theoretical curves, derived by the identification-plus-optimisation method. These results cover the frequency range 50Hz $\leqslant \omega_o \leqslant$ 180Hz. In all these cases a very good degree of fit is achieved.

In Fig.6, the final estimates of damping and inertial coefficients are presented, and compared with the corresponding short-bearing theoretical results, computed from the expressions given in Table 1. The damping coefficients shown here are the non-dimensional coefficients per land, defined by

$$B_{rr} = b_{rr} \frac{c^3}{2\pi n R \ell^3} \qquad (12)$$

and similarly for B_{ss}. In contrast the inertial coefficients, c_{rr} and c_{ss} are presented in dimensional form, and have the significance of hydrodynamic mass, m_H (in kg), for both lands. Results are presented for frequencies of vibration in the range 50 Hz to 180 Hz. It is noted that, in the experimental tests, when the frequency was varied all the other variables were maintained the same.

The experimentally determined coefficients, B_{rr} and B_{ss}, in Figs.6(a) and (b) respectively, are seen to be significantly greater in value than the theoretical values, by a factor of about 6, at low eccentricities. In both the radial and transverse directions the coefficients appear to be virtually independent of frequency. The tendency for the experimental coefficients to increase with increasing ϵ_o is reflected in the theoretical curves. Moreover, the experimental values of B_{rr} and B_{ss} are very similar, at low eccentricities, which again is in line with the theoretical predictions. Thus, qualitatively there is general agreement with the trends predicted by the short-bearing theory; this must, however, be set against the very poor quantitative agreement.

It is noted that, in previous work [15], a somewhat closer agreement between measured and theoretical values of B_{rr} and B_{ss} was obtained, although experimental values were, as here, significantly higher than the theoretical values. In Ref.[15] the circumferential groove used to supply lubricant to the squeeze-film was much deeper than that in the rig used in the present investigation. It is possible, therefore, that the geometry of the supply groove is an important factor in determining the magnitude of the damping coefficients. This is a factor which is not taken into account in the conventional theory, and requires further investigation.

The experimental inertial coefficients, shown in Fig.6(c) and (d), for the radial and transverse directions, respectively, show considerably more scatter than the corresponding damping results. This scatter is primarily due to the fact that the experimental value of the hydrodynamic

mass (of order 1 kg) is considerably less than the magnitude of the mechanical first mode mass, m (of order 10 kg). Thus, in computing c_{rr} from equation (6) (and similarly c_{ss}) δ^* is usually close to unity in value. This results in errors in the estimation of δ^* being magnified, by a factor of order 10, when c_{rr} and c_{ss} are computed.

Bearing in mind the relatively high level of uncertainty in the measured experimental inertial coefficients, it is possible to conclude that, with the possible exception of the results at 180Hz, there is little evidence of frequency dependency in the coefficients. The most significant feature of these results is that the experimental values of c_{rr} and c_{ss} are consistently much higher than the corresponding theoretical values, the discrepancy being typically about a factor of 10. In this respect the present results are fully in agreement with the results obtained in the earlier investigation of Ref.[15]. There, with a different geometry of squeeze-film damper, the experimental values of c_{rr} and c_{ss} were found to be, typically, about an order of magnitude higher than the corresponding short-bearing theoretical values.

In assessing these results it should also be borne in mind that, as mentioned earlier, each value of static eccentricity was achieved in two different ways; i.e. with the journal centre above, and below, the bearing centre. In the radial direction, the direction of pull, prior to release, was always upwards; thus differences between results obtained in these two, nominally similar, positions can be attributed to non-linear effects, arising from the use of a small, but finite, initial start amplitude, d^* (typically $d^* = 0.2$). The maximum discrepancies encountered were for the case of ω_o = 50Hz, and high values of ϵ_o; here the two values of c_{rr} were found to differ, by up to 100%, for ϵ_o = 0.3 to 0.5; these particular results must therefore be regarded as unreliable.

For the main body of the experimental results the vibration amplitudes were well within the linear regime of the squeeze-film. This was confirmed by performing tests at various start amplitudes. When normalised to unit initial displacement, the free decay curves were found to collapse, for different values of d^*, up to 0.2, indicating that a small motion (i.e. linear) model should be applicable. This is also confirmed by some results presented in Ref.15, where the linear regime of a squeeze-film was explored in more detail. As one would expect from physical reasoning, the degree of collapse tends to deteriorate as ϵ_o increases.

Returning to the overall results shown in Fig.6, it can be concluded that there are serious inadequacies in the conventional short-bearing theory for computing both damping and inertial coefficients. In this respect it is worth noting here that it has recently been shown that, due to inertial effects, large pressure variations can occur at the inlet to a squeeze-film bearing. This "Bernoulli effect", which is critically dependent on the details of the inlet groove geometry, is not taken into account in the conventional theory. In the present experiments, where a low viscosity lubricant was used, and no end seals were attached to the

bearing, the lubricant flow through rate was relatively high. In these circumstances one can anticipate that inlet inertial effects are likely to be significant, and may well account for the large discrepancies observed here between the measured force coefficients and the corresponding conventional theoretical estimates.

6 CONCLUSIONS

The main conclusions may be summarised as follows:

1. Damping and inertial coefficients can be estimated accurately, and efficiently, from digitised free-decay data. A combination of parametric identification and optimisation was found to result in theoretical curves which, in general, very closely matched the experimental data.

2. Both the measured damping and inertial coefficients were found to be significantly higher in magnitude than the corresponding values deduced from conventional short-bearing theory. In the case of inertial coefficients the observed discrepancy between theory and experiment supports the results of an earlier investigation [8].

3. Both the damping and inertial coefficients were found to be virtually independent of the frequency of vibration, over the frequency range 50Hz to 180Hz.

REFERENCES

1 Holmes, R. "The Damping Characteristics of Vibration Isolators used in Gas Turbines", Journal of Mechanical Engineering Science, Vol.19, No.6, 1977, pp.271-277.

2 Dogan, M. and Holmes, R., "Squeeze-Film Damping of Rotor-Dynamic Systems", The Shock and Vibration Bulletin, Vol.15, No.9, 1983, pp.3-8.

3. Hagg, A.C. and Sankey, G.O., "Some Dynamic Properties of Oil-Film Journal Bearings", Trans. ASME, Vol.23, 1956, pp.302-306.

4 Tichy J.A. "Effects of Fluid Inertia and Visco-elasticity on Squeeze-Film Bearing Forces" ASLE Trans., Vol.25, Part 1, January 1982, pp 125-132.

5 Tichy J.A. "Effects of Fluid Inertia and Visco-elasticity on Forces in the Infinite Squeeze-Film Bearing" ASLE Paper 83-AM-3E-1, 1983.

6 Tichy J.A. "The Effect of Fluid Inertia in Squeeze-Film Damper Bearings: A Heuristic and Physical Description" ASME Paper No 83-GT-177, 1983.

7 San Andrés L. & Vance J.M. "Effects of Fluid Inertia and Turbulence on Force Coefficients for Squeeze-Film Dampers" NASA publication CP 2338 (1984).

8 Reinhardt E. & Lund J.W. "The Influence of Fluid Inertia on the Dynamic Properties of Journal Bearings" Journal of Lubrication Technology, ASME, Vol.97, 1975, pp 159-175.

9 Szeri A.Z., Raimondi A.A. & Giron-Duarte A. "Linear Force Coefficients for Squeeze-Film Dampers" Journal of Lubrication Technology, ASME, Vol.195, 1983, pp 326-334.

10 Nelson C. "The Effect of Turbulence and Fluid Inertia on a Squeeze-Film Damper" AIAA/SAE/ASME 16th Joint Propulsion Conference, June 30-July 2, 1980.

11 Vance J. and Kirton A., "Experimental Measurement of the Dynamic Response of a Squeeze-Film Damper", Journal for Engineering in Industry, ASME, Vol.97, 1975, pp.1282-1286.

12 Tonnesen J., "Experimental Parametric Study of a Squeeze-Film Bearing", Journal of Lubrication Technology, ASME, Vol.98, 1976, pp.206-213.

13 Bansal P.N. and Hibner D.H., "Experimental and Analytical Investigation of Squeeze-Film Damper Forces Induced by Offset Circular Whirl Orbits", Journal of Mechanical Design, ASME, Vol.100, 1978, pp.549-557.

14 Thomsen K.K. and Anderson H., "Experimental Investigation of a Simple Squeeze-Film Damper", Journal of Engineering for Industry, ASME, Vol.96, 1974, pp.427-430.

15 Roberts J.B., Holmes R. & Mason P.J. "Estimation of

Squeeze-Film Damping and Inertial Coefficients from Experimental Free-Decay Data". Proceedings of the Institution of Mechanical Engineers, Engineering Sciences Division, Vol.200, No.2C, 1986, pp.123-133.

16 Holmes R. "The Vibration of a Rigid Shaft on Short Sleeve Bearings" J.Mech.Eng.Sci., Vol.2, 1960, pp 337-341.

17 Smith D.M. "Journal Bearing Dynamic Characteristics - Effect of Inertia of Lubricant" Proc. Inst. Mech. Engrs., Vol.179, Part 3J, 1964-65, pp 37-44.

18 Ramli M.D., Ellis J. & Roberts J.B. "On the Computation of Inertial Coefficients for Squeeze-Film Bearings" (to be published).

19 Mulcahy T.M., "Fluid Forces in Rods Vibrating in Finite Length Annular Regions", Journal of Applied Mechanics, ASME, Vol. 47, 1960, pp.234-240.

20 Brennen C., "On the Flow in an Annulus Surrounding a Whirling Cylinder", Journal of Fluid Mechanics, Vol.75, 1976, pp.173-191.

21 Detchmendy D.M. & Stridhar R. "Sequential Estimation of States and Parameters in Noisy Nonlinear Dynamical Systems" Trans.ASME, Journal of Basic Engineering, Vol.16, 1966, pp 363-368.

22 Johnson R.C., "Mechanical Design Synthesis", Second Edition, R.E. Krieger Publishing Company, Huntington, New York, 1978, pp.423-431.

23 Tichy J.A. and Bourgin P., "The Effect of Inertia in Lubrication Flow Including Entrance and Initial Conditions", Journal of Applied Mechanics, ASME, Vol.52, 1985, pp.759-765.

24 Tichy J.A. and Chen S.H., "Plane Slider Bearing Load Due to Fluid Inertia - Experiment and Theory", Journal of Tribology, ASME, Vol.107, 1985, pp.33-39.

Theoretical Short-Bearing Coefficients

	Damping Coefficients	Inertial Coefficients
Radial	$b_{rr} = \left(\frac{\pi\eta R\ell^3}{c^3}\right) \frac{(1 + 2\varepsilon_o^2)}{(1 - \varepsilon_o^2)^{5/2}}$	$c_{rr} = \frac{\pi\rho R\ell^3}{12c} \left\{\frac{2}{\varepsilon_o^2} \left[\frac{1}{(1 - \varepsilon_o^2)^{\frac{1}{2}}} - 1\right]\right\}$
Transverse	$b_{ss} = \left(\frac{\pi\eta R\ell^3}{c^3}\right) \frac{1}{(1 - \varepsilon_o^2)^{3/2}}$	$c_{ss} = \frac{\pi\rho R\ell^3}{12c} \left\{\frac{2}{\varepsilon_o^2} \left[1 - (1 - \varepsilon_o^2)^{\frac{1}{2}}\right]\right\}$

Table 1

Comparison between identification and optimisation results, for two different sampling intervals

Δt = 0.5ms

Eccentricity ϵ_o	mean square error (e)		percentage difference
	identified(1)	optimised(2)	
0.0	0.170	0.129	24
0.1	0.103	0.063	39
0.2	0.189	0.130	31
0.3	0.152	0.072	52
0.4	0.133	0.069	48
0.5	0.129	0.105	18

Δt = 0.25ms

Eccentricity ϵ_o	mean square error (e)		percentage difference
	identified(1)	optimised(2)	
0.0	0.067	0.065	3
0.1	0.086	0.076	12
0.2	0.090	0.084	6
0.3	0.090	0.088	2
0.4	0.050	0.047	5
0.5	0.079	0.070	12

$$\text{percentage difference} = \frac{1}{e_1} (e_1 - e_2) \times 100$$

Table 2

Repeatability results

Parameters obtained from individual tests

Test No	γ^*	ε^*	percentage difference γ^*_{PD}	percentage difference ε^*_{PD}
1	0.563	0.908	-2.6	-0.1
2	0.550	0.897	-0.2	1.2
3	0.547	0.894	-0.3	1.5
4	0.559	0.897	-1.8	1.1
5	0.547	0.896	0.3	1.3
Av.	0.553	0.898	-0.7	1.0

Parameters obtained from averaged data

γ^*_{AV}	ε^*_{AV}
0.549	0.907

$$\gamma^*_{PD} = \frac{1}{\gamma^*_{AV}} (\gamma^*_{AV} - \gamma^*) \times 100$$

$$\varepsilon^*_{PD} = \frac{1}{\varepsilon^*_{AV}} (\varepsilon^*_{AV} - \varepsilon^*) \times 100$$

Table 3

PART TWO: THEORETICAL INVESTIGATIONS

NOTATION

a_{rr}, a_{ss}	direct fluid-film stiffness coefficients for the radial and the transverse directions, respectively
a_{rs}, a_{sr}	cross fluid-film stiffness coefficients for the radial and the transverse directions
a	matrix containing the fluid-film stiffness coefficients a_{rr} . . . a_{ss}
b_{rr}, b_{ss}	direct fluid film damping coefficients, for the radial and transverse directions, respectively
b_{rs}, b_{sr}	cross fluid-film damping coefficients, for the radial and transverse directions.
b	matrix containing the fluid-film damping coefficients b_{ss} . . . b_{rr}
c	radial clearance between the journal and the bearing
c_{rr}, c_{sr}	direct fluid-film inertial coefficients for the radial and transverse directions, respectively
c_{rs}, c_{ss}	cross fluid-film inertial coefficients for the radial and transverse directions
c_{rr}', c_{ss}'	non-dimensional direct fluid-film inertial coefficients defined by equation (16)
c_{rr}'', c_{ss}''	non-dimensional direct fluid-film inertial coefficients defined by equation (22)
c^*_{rr} , c^*_{ss}	non-dimensional direct fluid-film inertial coefficients defined by equation (26)
c	matrix containing the fluid-film inertial coefficients c_{ss} . . . . c_{rr}
D	diameter of the journal
e	eccentricity of the journal
$f_r'(e,z), f_s'(e,z)$	functions of e and z, defined in equation (7)
L	land length of the bearing
F_r, F_s	fluid-film forces, in the radial and transverse directions, respectively
F	column matrix containing F_r and F_s

F_r', F_s'	non-dimensional fluid-film forces, due to inertial effects, in the radial and transverse directions, respectively
$p(\theta,z)$	fluid-film pressure, arising from inertial effects
$p'(\theta,z)$	non-dimensional fluid-film pressure, arising from inertial effects ($p' = p/\rho\omega^2R^2$)
x_r, x_s	journal displacement in the radial and transverse directions, respectively
Z	axial distance within the film
z	non-dimensional axial distance ($z = Z/L$)
α_r, α_s	acceleration of the journal in the radial and transverse directions, respectively
α_r', α_s'	non-dimensional acceleration of the journal ($\alpha_r' = \alpha_r/\omega^2c$, $\alpha_s' = \alpha_s/\omega^2c$)
ϵ_o	static eccentricity ratio (e/c)
Φ	attitude angle
μ	absolute viscosity of squeeze-film fluid
ρ	density of squeeze-film fluid
θ	angular position, measured from position of maximum film thickness
ω	frequency of vibration

SUMMARY

Inertial coefficients for full squeeze film bearings are evaluated theoretically using Smith's differential equation relating fluid film pressure to journal acceleration [1]. The variations of the non-dimensionalised inertial coefficients with static eccentricity ratio in the radial and transverse directions are compared with some corresponding values obtained from Reinhardt and Lund [2] and Szeri et al [3].

The results from these three methods show good agreement, especially for short bearings, (i.e. bearings with low values of length-to-diameter ratio). However, Smith's approach has the advantage of computational simplicity and leads to fairly simple, asymptotic, analytical expressions for very short, and very long, bearings.

1. INTRODUCTION

Squeeze-film dampers have proved a particularly useful device for controlling the stability, and synchronous response, of the rotating shafts which occur in turbomachinery. In such machinery there has been a tendency, in recent years, to increase size and rotational speed, and to use light oils, of low viscosity. All these factors have resulted in increases in the value of the gap Reynolds number

$$Re = \frac{\rho\omega c^2}{\eta} = \frac{\text{fluid inertia force}}{\text{fluid viscous force}}$$

at which squeeze-film dampers operate in practice; values of Re of order one, or greater, are in fact now common. In this situation one can expect inertial dynamic effects to be significant. Recent theoretical studies [1-8] and experimental investigations [9-12] have indeed confirmed the important influence of fluid inertia in squeeze-film dynamic behaviour.

For small motions of the squeeze-film journal, within its clearance circle, it is possible to linearise the equations of motion and to represent the dynamic behaviour of the squeeze-film in terms of damping and inertial coefficients. Theoretical methods of evaluating the damping coefficients, by using Reynolds equation, have been known for many years but it is only recently that the problem of evaluating the inertial coefficients theoretically has received much attention.

Two theoretical approaches to this problem have been reported fairly recently by Reinhardt and Lund [2] and Szeri et al [3]. In ref [2] a perturbation technique is used to predict values for the inertial coefficients of a bearing with a finite length-to-diameter (L/D) ratio. Numerical values of these coefficients are obtained for various values of static eccentricity ratio, ϵ_o, and for L/D values of 0.1, 0.5 and 1. In the treatment of Szeri et al [3] an alternative approximate analysis, derived from the full Navier-Stokes equations for fluid flow, is also used to compute values of the inertial coefficients for different values of ϵ_o and L/D. Their analysis requires, at one stage, the assumption that L/D is

small.

Both the theoretical treatments of refs [2] and [3] are involved and lengthy; the resulting computation procedures for evaluating the inertial coefficients are correspondingly complex and time-consuming. There is, however, a much simpler, alternative theoretical approach, first proposed by Smith [1], which leads, in turn, to much simpler calculations. This approach results in a fairly simple differential equation for the pressure field in a lubricant film, as the result of journal acceleration; in form this equation is similar to the familiar two-dimensional Reynolds equation for finite squeeze-film bearings. Smith did not attempt a numerical solution of this differential equation, with a view to evaluating inertial coefficients for finite L/D values, but for the asymptotic cases of $L/D \to 0$ (short bearings) and $L/D \to \infty$ (long bearings), he was able to deduce simple analytical expressions for these coefficients. However, despite it's importance, Smith's approach appears to have gone largely unnoticed by workers in the area of squeeze-film behaviour.

The objective of this paper is threefold: firstly to draw attention to the relevance of Smith's work in the context of squeeze-film dampers; secondly to obtain values of the inertial coefficients, for finite L/D ratios, by numerically solving Smith's pressure differential equation; and thirdly, to compare these numerical values with the corresponding values given in refs [2] and [3].

2. THEORY

2.1 Hydrodynamic forces

An examination of the fluid reaction forces on an oscillating body, moving in an incompressible fluid, indicates that they depend on its displacement, velocity and acceleration. Assuming that these forces depend only on the instantaneous motion in two orthogonal directions (here taken to be the radial and transverse directions, r and s respectively), the general linearised expresssions for the hydrodynamic forces, F_r and F_s, for small movements of the body are, in matrix form, as follows [1]

$$F = ax + b\dot{x} + c\ddot{x} \qquad (1)$$

where

$$F = \begin{matrix} F_r \\ F_s \end{matrix} \qquad x = \begin{matrix} x_r \\ x_s \end{matrix} \qquad (2)$$

$$a = \begin{matrix} a_{rr} & a_{rs} \\ a_{sr} & a_{ss} \end{matrix} \qquad (3)$$

$$b = \begin{matrix} b_{rr} & b_{rs} \\ b_{sr} & b_{ss} \end{matrix} \qquad (4)$$

and

$$c = \begin{matrix} c_{rr} & c_{rs} \\ c_{sr} & c_{ss} \end{matrix} \qquad (5)$$

Under full-film conditions, (i.e. no starvation, or cavitation), the cross-terms disappear; in other words, the

matrices $\underline{a}$, $\underline{b}$ and $\underline{c}$ are diagonal. Furthermore, all the terms in $\underline{a}$ are negligible [1]. $\underline{b}$ and $\underline{c}$ contain, respectively, the damping and inertial coefficients.

2.2 The inertial coefficients

A linearised approach to the evaluation of a squeeze-film fluid forces allows a separate evaluation of the inertia coefficients which arise from the effect of the journal acceleration.

Smith [1] has shown that if α'_r and α'_s are the non-dimensional journal accelerations in the radial ($\alpha'_r = x_r/\omega^2 c$) and the transverse ($\alpha'_s = x_s/\omega^2 c$) directions respectively, the non-dimensional fluid pressure p' arising from inertial effects, is governed by the following differential equation

$$\frac{\partial}{\partial\theta}\left[(1 + \epsilon_o \cos\theta)\frac{\partial p'}{\partial\theta}\right] + \left(\frac{R}{L}\right)^2(1 + \epsilon_o\cos\theta)\frac{\partial^2 p'}{\partial z^2}$$

$$= \alpha_r' \cos\theta + \alpha_s' \sin\theta \qquad (6)$$

This equation is similar to the two-dimensional Reynolds equation for the pressure distribution due to viscous effects alone. Here, θ is the angle measured from the attitude angle ($\theta = 0$ at maximum film thickness), z is the non-dimensional axial position within the fluid-film, and ϵ_o is the static eccentricity ratio (refer to Fig.1).

The solution to equation (6), subject to appropriate boundary conditions is a pressure field, $p(\theta,z)$ which depends linearly on α_r' and α_s'. The general solution is of the form

$$p'(\theta,z) = f_r'(\theta,z)\alpha_r' + f_s'(\theta,z)\alpha_s' \qquad (7)$$

The fluid inertial forces F'_r and F'_s (defined as positive when applied as compressive force between the journal and the bearing) may be evaluated by suitable integrations of the pressure field. Thus, these forces are given by:

$$F'_r = -\int_A\int p'(\theta,z)\cos\theta\, d\theta\, dz \qquad (8)$$

$$F'_s = -\int_A\int p'(\theta,z)\sin\theta\, d\theta\, dz \qquad (9)$$

where integration is over the whole pressure field.

It follows from the form of equations (7), (8) and (9) that

$$F_r' = c_{rr}'\alpha_r' + c_{rs}'\alpha_s' \qquad (10)$$

$$F_s' = c_{sr}' \alpha_r' + c_{ss}' \alpha_s' \qquad (11)$$

where the non-dimensional inertial coefficients are given by

$$c_{rr}' = - \int_A \int f_r'(\theta,z) \cos\theta \, d\theta \, dz \qquad (12)$$

$$c_{rs}' = - \int_A \int f_s'(\theta,z) \cos\theta \, d\theta \, dz \qquad (13)$$

$$c_{sr}' = - \int_A \int f_r'(\theta,z) \sin\theta \, d\theta \, dz \qquad (14)$$

$$c_{ss}' = - \int_A \int f_s'(\theta,z) \sin\theta \, d\theta \, dz \qquad (15)$$

2.2.1 Evaluation of inertial coefficients for finite bearings

The general pressure differential equation (equation (6)), was solved numerically using a five point finite different approximation for the differentials of the equation in the θ (circumferential) and z (axial) directions for a range of length to diameter ratios and static eccentricity ratios.

The large set of coupled linear equations in nodal pressure was solved using an iterative technique. Depending on the trial length to diameter ratio, with the demarcation arbitrarily set at L/D = 3, the nodal pressure field was set initially to the Smith analytical values for either short or long bearings (the short bearing solution is given here as equation (18)). The iteration sequence was terminated when the percentage change in all nodal pressures during one iteration was less than 0.1.

It was assumed that the bearing consisted of two identical lands, of length L, separated by a central circumferential groove, through which the lubricant was supplied. It was also assumed that the lubricant was free to discharge to atmospheric pressure at the bearing outlets. The fluid film pressure arising from inertial effects was taken to be zero at both the supply groove and at the discharge edges.

Using the non-dimensional, nodal, pressure field and with integration over the full land width axially, and over 2π (for a full film) circumferentially, equations (8) and (9) were integrated numerically using a variant Simpson's rule to determine the non-dimensional fluid-film forces due to inertial effects. Equations (10) and (11) were then used to determine the non-dimensional direct fluid-film inertial coefficients, c_{rr}' and c_{ss}'. For all the investigated geometries, repeated numerical trials were made with finer finite difference grids until stable inertial coefficient values were obtained. Generally more grid points were needed to achieve stable coefficient values for long bearings.

It should be noted that c_{rr}' and c_{ss}' can be converted to

dimensional form as follows:

$$c_{rr} = \rho \frac{R^3 L}{c} c'_{rr} , \qquad c_{ss} = \rho \frac{R^3 L}{c} c'_{ss} \tag{16}$$

where c_{rr} and c_{ss} have the physical significance of equivalent hydrodynamic masses. For comparison with the theoretical results of other workers and with Smith's short and long bearing analytical solutions, the inertial coefficients were further normalized according to equations (21) or (26) depending on the trial geometry length to diameter ratio. The demarcation length to diameter ratio was taken arbitrarily at 3. The comparisons with the results of Reinhardt and Lund, and Szeri et al, thus all fall in the short bearing category.

3. COMPARISON OF RESULTS

3.1 Short bearings

Returning to the general differential pressure relationship given by equation (6), it is observed that, for a short bearing (i.e. $L/D \ll 1$) the pressure gradient in the z direction will dominate over that in the circumferential direction. In these circumstances equation (6) may be approximated by

$$\left(\frac{R}{L}\right)^2 (1 + \epsilon_o \cos\theta) \frac{\partial^2 p'}{\partial z^2} = \alpha_r' \cos\theta + \alpha_s' \sin\theta \tag{17}$$

On integration this equation gives the result

$$p'(\theta,z) = \frac{1}{2} \left(\frac{L}{R}\right)^2 (z^2 - \frac{1}{4}) \left[\frac{\alpha_r' \cos\theta}{1+\epsilon_o\cos\theta} + \frac{\alpha_s' \sin\theta}{1+\epsilon_o\cos\theta} \right] \tag{18}$$

The coefficients in equations (12) and (15) may now be evaluated analytically; the result is

$$c'_{rr} = \left(\frac{L}{R}\right)^2 \frac{\pi}{12} \frac{2}{\epsilon_o^2} \left[\frac{1}{(1 - \epsilon^2)^{1/2}} - 1 \right] \tag{19}$$

$$c'_{ss} = \left(\frac{L}{R}\right)^2 \frac{\pi}{12} \frac{2}{\epsilon_o^2} \left[1 - (1 - \epsilon_o^2)^{1/2} \right] \tag{20}$$

For the present purposes it is convenient to introduce the non-dimensional coefficients

$$c''_{rr} = \frac{12}{\pi} \left(\frac{R}{L}\right)^2 c'_{rr} \qquad c''_{ss} = \frac{12}{\pi} \left(\frac{R}{L}\right)^2 c'_{ss} \tag{21}$$

Equations (19) and (20) may then be rewritten as

$$c''_{rr} = \frac{2}{\epsilon_o^2} \left[\frac{1}{(1 - \epsilon_o^2)^{1/2}} - 1 \right] \tag{22}$$

$$c_{ss}'' = \frac{2}{\epsilon_o^2}\left[1 - (1 - \epsilon_o^2)^{1/2}\right] \qquad (23)$$

for the non-dimensional coefficients c_{rr}'' and c_{ss}''. In the limiting case, as $\epsilon_o \to 0$, $c_{rr}'' = c_{ss}'' = 1$.

The numerically evaluated inertial coefficients c_{rr}' and c_{ss}' for finite bearings (see section 2) are conveniently converted into the non-dimensional coefficients c_{rr}'' and c_{ss}'', respectively, for the purposes of comparison with the short-bearing results given by equations (22) and (23). Clearly, one can expect the inertial coefficients evaluated from the finite difference solution to approach the values evaluated from equations (22) and (23) for low values of L/D ratio in both the radial and transverse directions.

In Figs. 2 to 6 the variation of c_{rr}'' and c_{ss}'', respectively, with ϵ_o are shown, for L/D values ranging from 0.1 to 2.0. In each case the result obtained by a numerical solution of equation (6) is compared with the asymptotic results, for $L/D \to 0$, as given by equations (22) and (23). Comparisons are also made with the results presented by Reinhardt and Lund [2] (values given for L/D = 0.1, 0.5 and 1.0) and Szeri et al [3] (values given for L/D = 0.1, 0.2, 0.5, 1.0 and 2.0).

It is observed that, for L/D = 0.1 and 0.5, the values of the coefficients obtained from the different methods compare reasonably well, especially for the transverse direction. However, for the same L/D value, the coefficient values obtained from ref.[2] are slightly higher, in the radial direction. The agreement tends to deteriorate as L/D increases, as the results for L/D = 1 demonstrate. The results of Szeri et al [3] agree very closely with the present results, for L/D = 0.1, 0.2 and 0.5; figs. 2 to 4 show that there is virtually exact agreement, in this range.

The difference between the present results and Szeri et al's results, tends to increase, as L/D increases. This is seen clearly by the comparison of results for L/D = 2.0 (fig.6). This discrepancy is not surprising, since Szeri et al [3] introduce the assumption that L/D is small, at one stage in their analysis. Their results for L/D > 1 are thus likely to be less accurate than the present values.

It is noted that the coefficient values obtained from refs. [2] and [3] were found by reading values from graphs; small numerical errors are inevitably introduced, in this process.

3.2 Long bearings

For the long bearings (L/D >> 1), the pressure gradient in the circumferential direction is dominant and the general pressure differential relationship of equation (6) can be approximated as

$$\frac{\partial}{\partial\theta}[(1 + \epsilon_o \cos\theta)\frac{\partial p'}{\partial\theta})] = \alpha_r' \cos\theta + \alpha_s' \sin\theta \qquad (24)$$

This can be solved analytically. Following the procedure in section 3, one obtains analytical expressions for the inertial coefficients; thus

$$c_{rr}' = c_{ss}' = \pi \frac{2}{\epsilon_o^2}[1 - (1 - \epsilon_o^2)^{1/2}] \qquad (25)$$

Here it is convenient to scale the coefficients so that the theoretical values are unity, at $\epsilon_o = 0$. Accordingly, the non-dimensional coefficients

$$c_{rr}^* = \frac{c_{rr}'}{\pi}, \qquad c_{ss}^* = \frac{c_{ss}'}{\pi} \qquad (26)$$

are introduced here. Thus, from equation (25)

$$c_{rr}^* = c_{ss}^* = \frac{2}{\epsilon_o^2}[1 - (1 - \epsilon_o^2)^{1/2}] \qquad (27)$$

for the asymptotic case $L/D \to \infty$. For large L/D values, the present numerical values of the inertial coefficients c_{rr}' and c_{ss}' (see section 2) will be converted to c_{rr}^* and c_{ss}^*, for comparison with equation (27).

Fig.7 shows the variation of the inertial coefficients with static eccentricity ratio for different values of L/D ratios, as compared to the approximate long bearing solution for $L/D \to \infty$, for the radial and transverse directions.

At high values of L/D ratio the numerical values of the inertial coefficients approach the long bearing approximation As the L/D ratio decreases, the difference in the inertial values becomes greater as shown by fig.7.

4. CONCLUSION

It has been shown that numerical values of the inertial coefficients, for both the radial and transverse directions, can be obtained in a simple way by numerically solving a partial differential equation for the pressure field generated by journal acceleration. The numerical values obtained were found to converge towards the results obtained from simple asymptotic expressions, for both $L/D \to 0$ and $L/D \to \infty$. The results presented here enable the accuracy and range of validity of these asymptotic results to be assessed. A comparison with some results obtained by the more elaborate analyses of Reinhardt and Lund [2] and Szeri et al [3] indicates that the present approach yields results of comparable accuracy, but with much less computational effort.

REFERENCES

1. Smith, D.M. "Journal Bearing Dynamic Characteristics - Effect of Inertia of Lubricant", Proc. Inst.Mech.Engs., Vol.179, Part 3J, 1964-1965, pp.37-44.

2. Reinhardt, E. and Lund, J.W., "The Influence of Fluid Inertia on the Dynamic Properties of Journal Bearings", Journal of Lubrication Technology, ASME, Vol.97,1975 pp 159-175.

3. Szeri, A.Z., Raimondi, A.A. and Giran-Durante,A. "Linear Force Coefficients for Squeeze-Film Dampers". Journal of Lubrication Technology, ASME, Vol. 195, 1983, pp.326-334.

4. Tichy, J.A. "Effect of Fluid Inertia and Viscoelasticity on Squeeze-Film Bearing Forces", ASLE Trans., Vol.25, Part 1, January 1982, pp.125-132.

5. Tichy, J.A. "Effects of Fluid Inertia and Viscoelasticity on Forces in the Infinite Squeeze-Film Bearing, ASLE Paper 83-AM-2E-1, 1983.

6. Constantinescu, V.N. "On the Influence of Inertia Forces in Turbulent and Laminar Self-Acting Films", Journal of Lubrication Technology, ASME, July 1970, pp.473-479.

7. Tichy, J.A., "The Effect of Fluid Inertia on Squeeze-Film Damper Bearings: A Heuristic and Physical Description", ASME Paper No. 83-GT-177, 1983.

8. San Andres, L. and Vance, J.M. "Effects of Fluid Inertia and Turbulence on Force Coefficients for Squeeze-Film Dampers", NASA Publication CP 2338, 1984.

9. Kuzma, D.A. "Fluid Inertia Effects in Squeeze Films", App.Sci.Res., Vol.18, Aug.1967, pp.15-20.

10. Burton, R.A. and Carper, H.J. "An Experimental Study of Annular Flows with Application in Turbulent Film Lubrication", Journal of Lubrication Technology, ASME, Series F. Vol..89, July 1967, pp.381-391.

11. Roberts, J.B., Holmes, R. and Mason, P.J., "Estimation of Squeeze-Film Damping and Inertial Coefficients from Experimental Free-Decay Data", to be published in the Proceedings of the Institution of Mechanical Engineers, Engineering Science Division, UK, 1986.

12. Tichy, J.A. "Measurement of Squeeze-Film Bearings Forces to Demonstrate the Effects of Fluid Inertia", ASME Paper No. 84-GT-11,1984.

CONCLUDING REMARKS

This investigation has revealed that the damping and inertial coefficients of a squeeze-film bearing are, at least in some circumstances, substantially higher than the values predicted from conventional hydrodynamic theory. Thus, to enable the formulation of adequate design procedures for these devices, it is essential that the source of the discrepancy between theory and experiment be identified and rectified.

To resolve this problem it is suggested that the present investigation, described here, be extended to determine those operating parameters which have a major, controlling influence over the discrepancy between theory and experiment. It is likely that the inlet geometry, and the viscosity of the lubricant, play an important role. For example, in the work described here the flow-through rate of the lubricant was high, due to the use of a low viscosity lubricant. With high axial flow velocities the inertial effects at the squeeze-film inlet are likely to be important, and may well be dominant for a short bearing. Clearly, changing the inlet goemetry, or the lubricant viscosity, would have a pronounced influence of the magnitude of the inlet dynamic effect. This effect is not taken into account in present design methods.

Such an investigation would be most effectively carried out using a forced vibration test method, in conjunction with parametric identification techniques. From forced vibration test results one could, for example, discriminate between mass (or inertial) and stiffness coefficients, and could identify damping parameters even when the damping factor is greater than the critical value - i.e. the case "overdamped" vibration. Thus one would obtain results for a wide range of lubricant viscosities, in a rapid and efficient manner. Such work would involve the development of new software for parametric identification, and some modifications to the experimental rig. For example, it would be necessary to incorporate a force transducer, and to simultaneously capture two channels of information - displacement response and force input.

In parallel with this work, a more detailed experimental investigation of the lubricant flow within a squeeze-film would be highly beneficial. The most promising avenue for research here would seem to be the measurement of dynamic pressure variations. Through investigations of the variation of the instantaneous pressure distribution with time it should be possible to pin-point the source of discrepancy between theory and experiment.

Finally, fundamental theoretical studies of the flow within squeeze-film are required, which take proper account of inlet and outlet effects.

Acknowledgement

This work was funded by the U.S. Army European Research Office, under Grant No. DAJA45-84-C-004. The authors gratefully acknowledge this support.

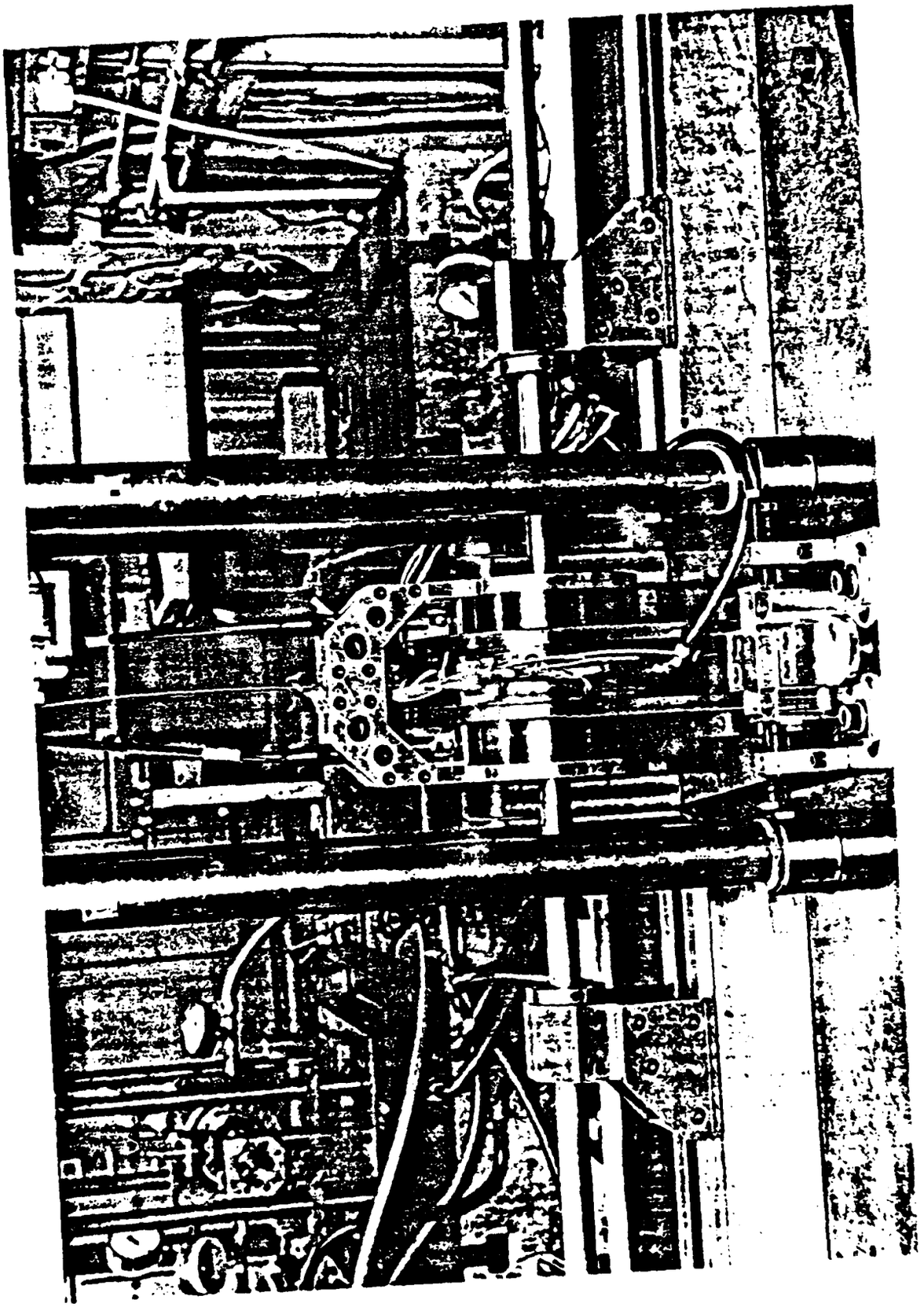

Fig. 1(a)

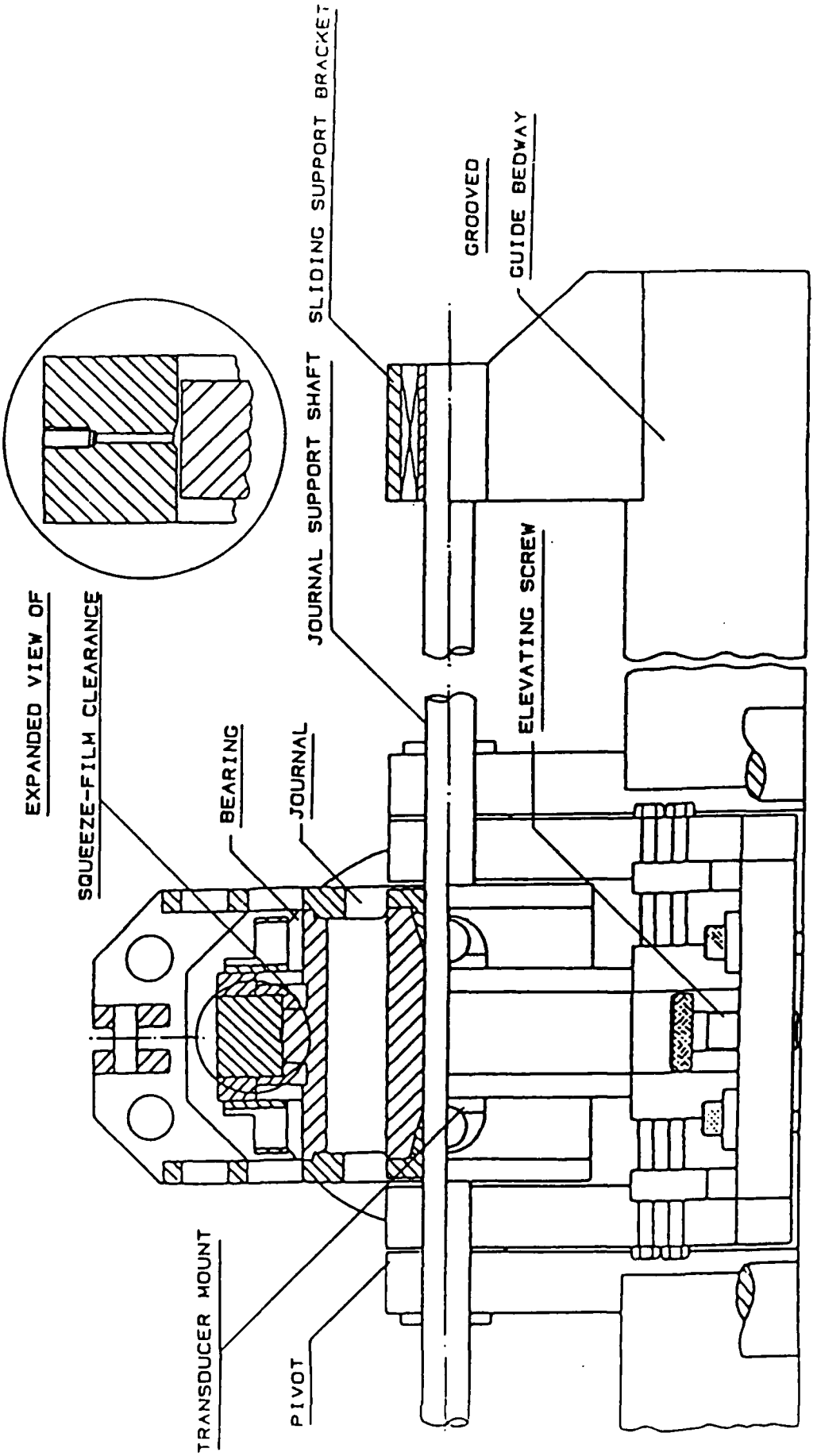
EXPANDED VIEW OF
SQUEEZE-FILM CLEARANCE
BEARING
JOURNAL
TRANSDUCER MOUNT
PIVOT
JOURNAL SUPPORT SHAFT
SLIDING SUPPORT BRACKET
GROOVED
GUIDE BEDWAY
ELEVATING SCREW

Fig. 1(b)

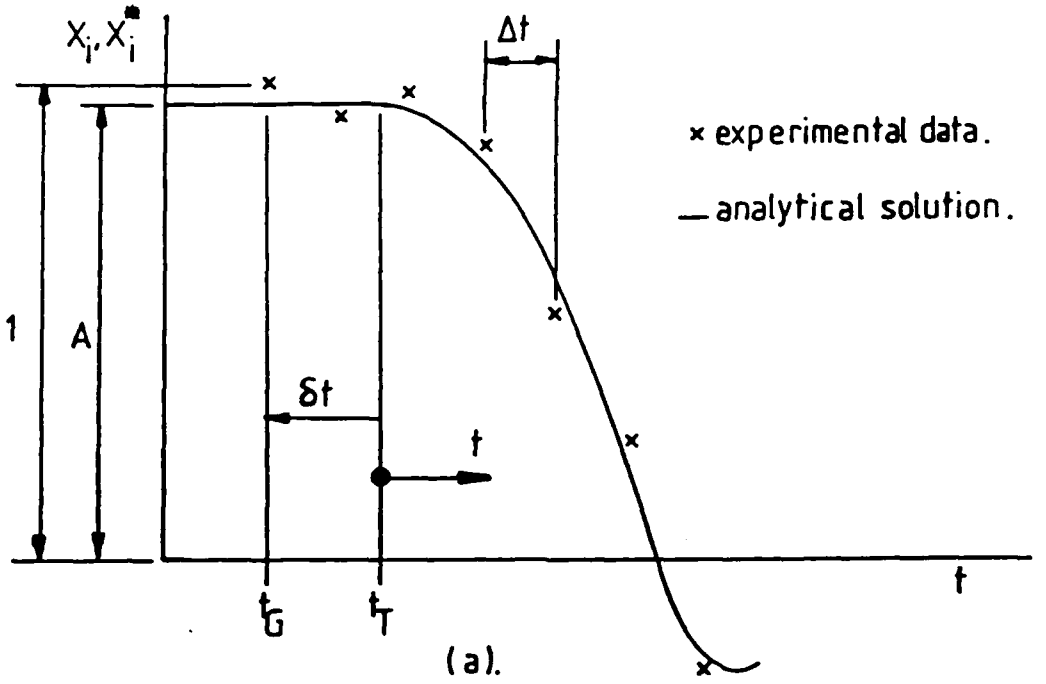

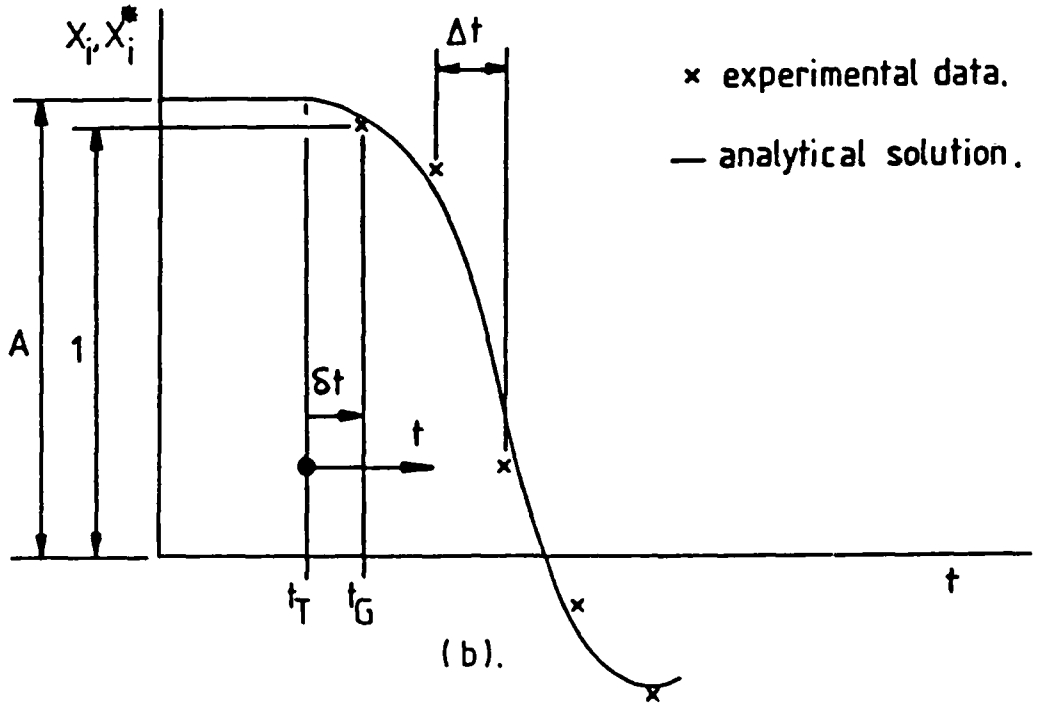

FIG. 2 OPTIMAL FIT TO EXPERIMENTAL DATA.

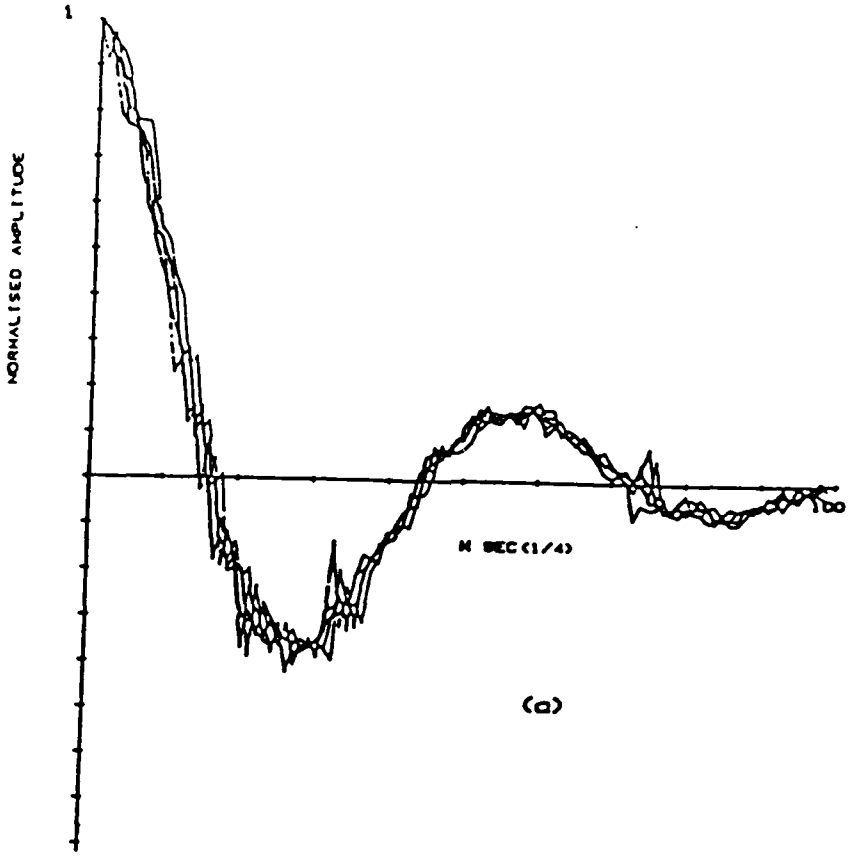
1
NORMALISED AMPLITUDE
100
M SEC (1/4)

(a)

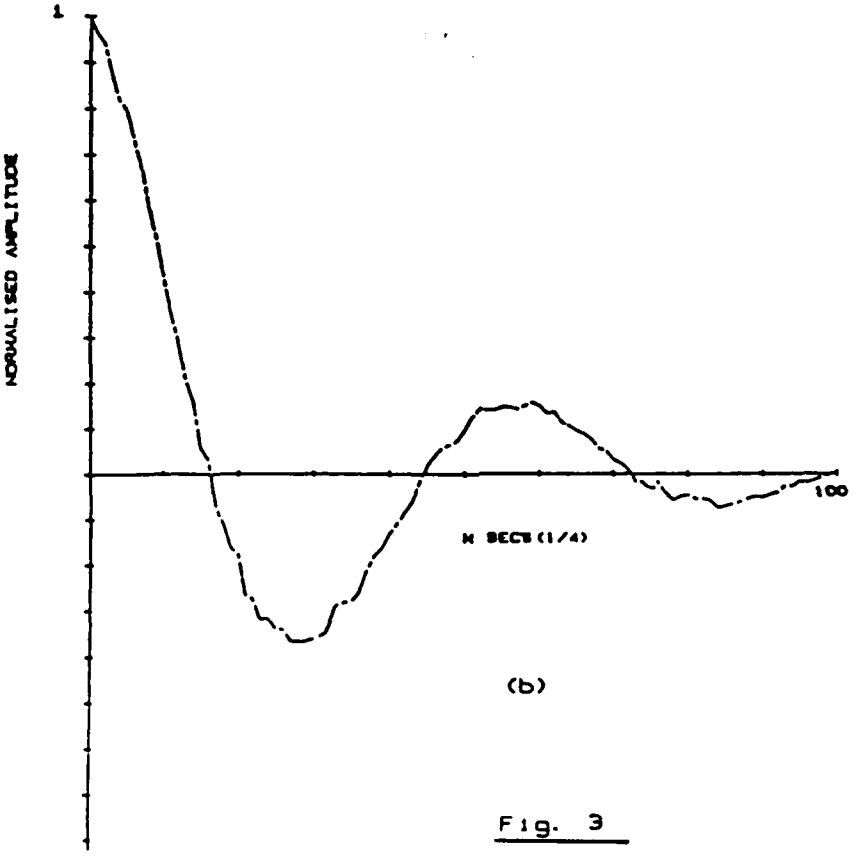
1
NORMALISED AMPLITUDE
100
M SECS (1/4)

(b)

Fig. 3

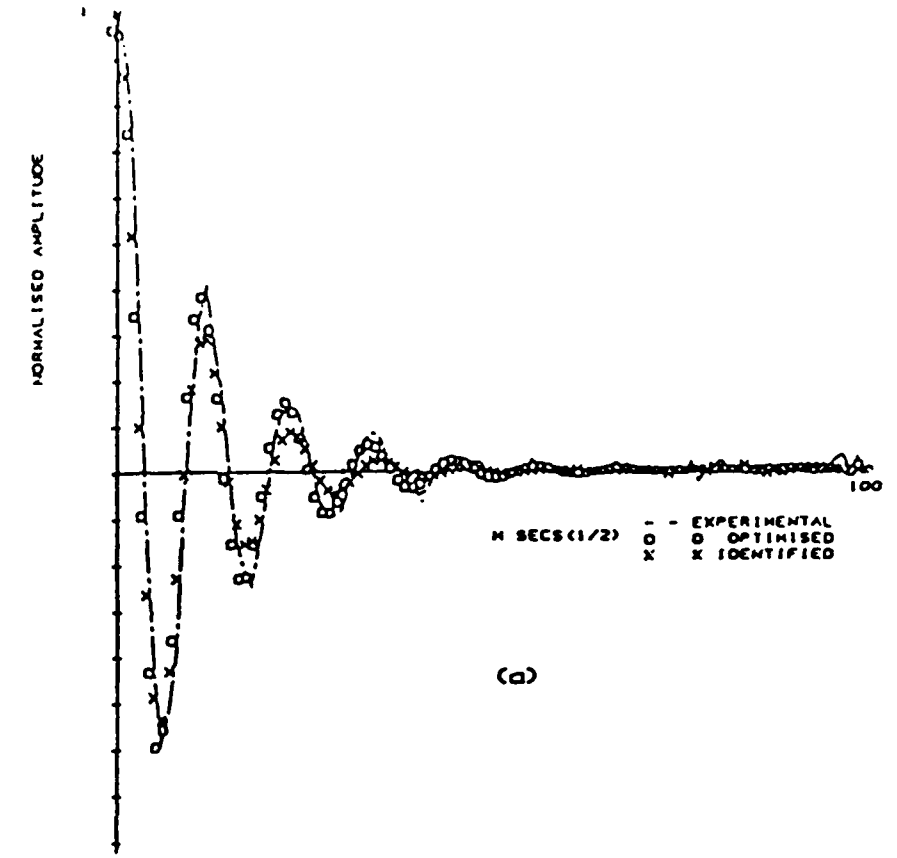
NORMALISED AMPLITUDE
100
H SECS(1/2)
- - EXPERIMENTAL
O O OPTIMISED
X X IDENTIFIED

(a)

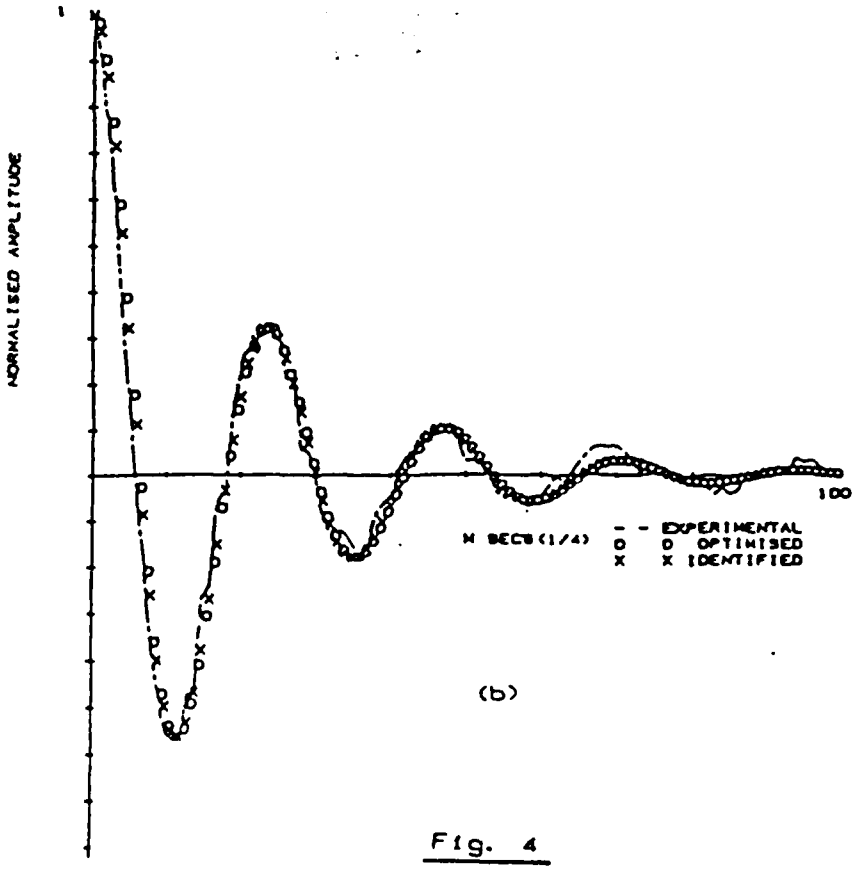
NORMALISED AMPLITUDE
100
H SECS(1/4)
- - EXPERIMENTAL
O O OPTIMISED
X X IDENTIFIED

(b)

Fig. 4

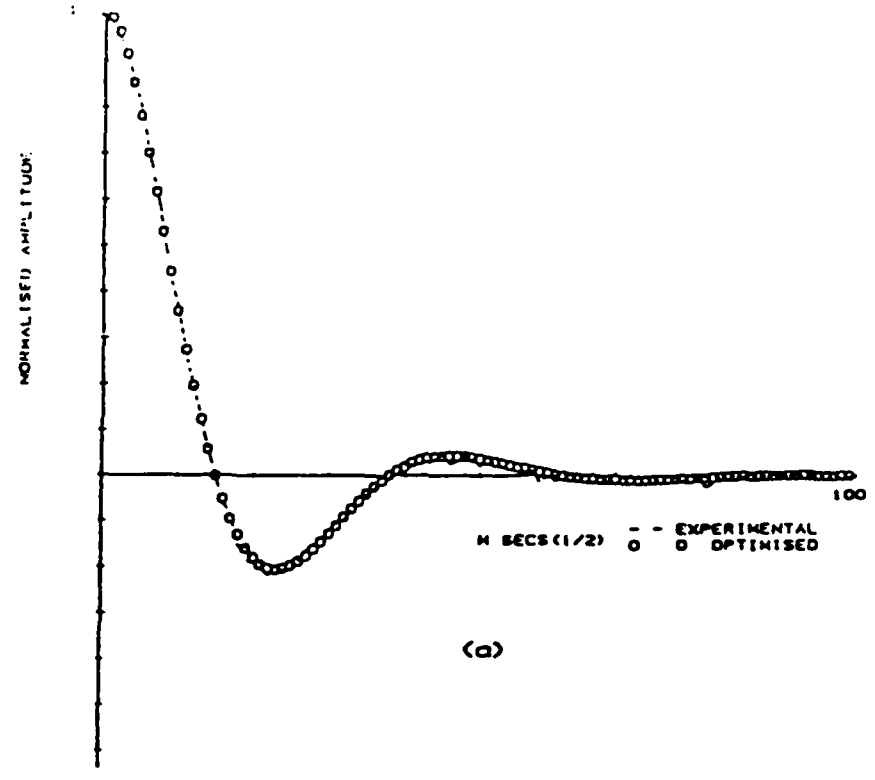
NORMALISED AMPLITUDE
100
M SECS (1/2)
EXPERIMENTAL
OPTIMISED
(a)

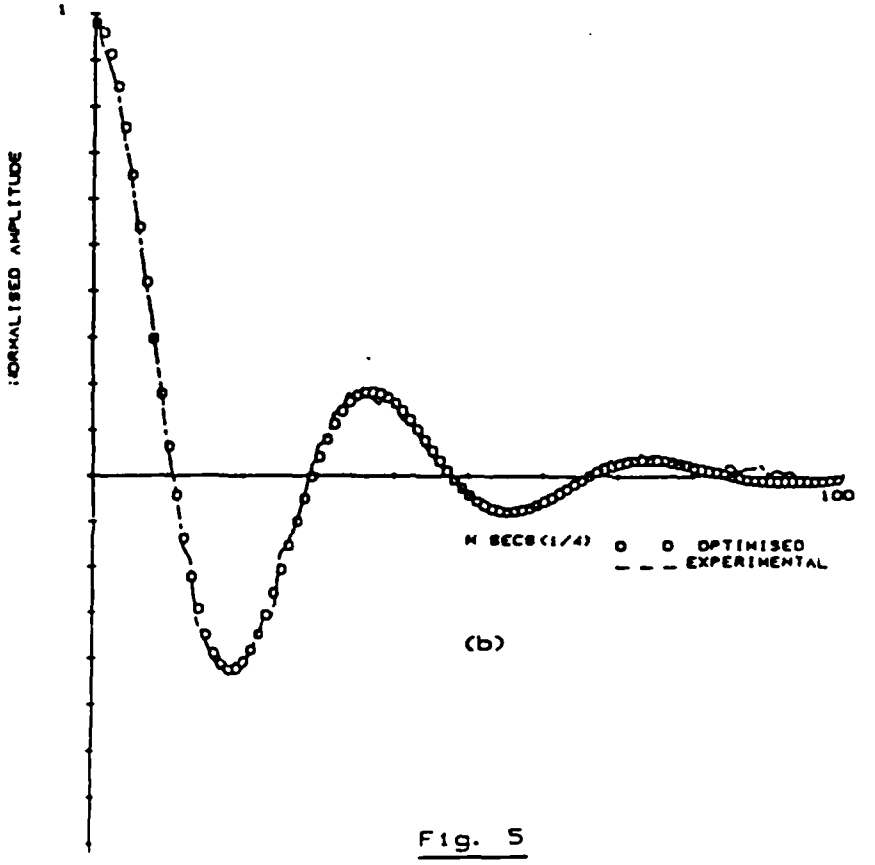
NORMALISED AMPLITUDE
100
M SECS (1/4)
OPTIMISED
EXPERIMENTAL
(b)

Fig. 5

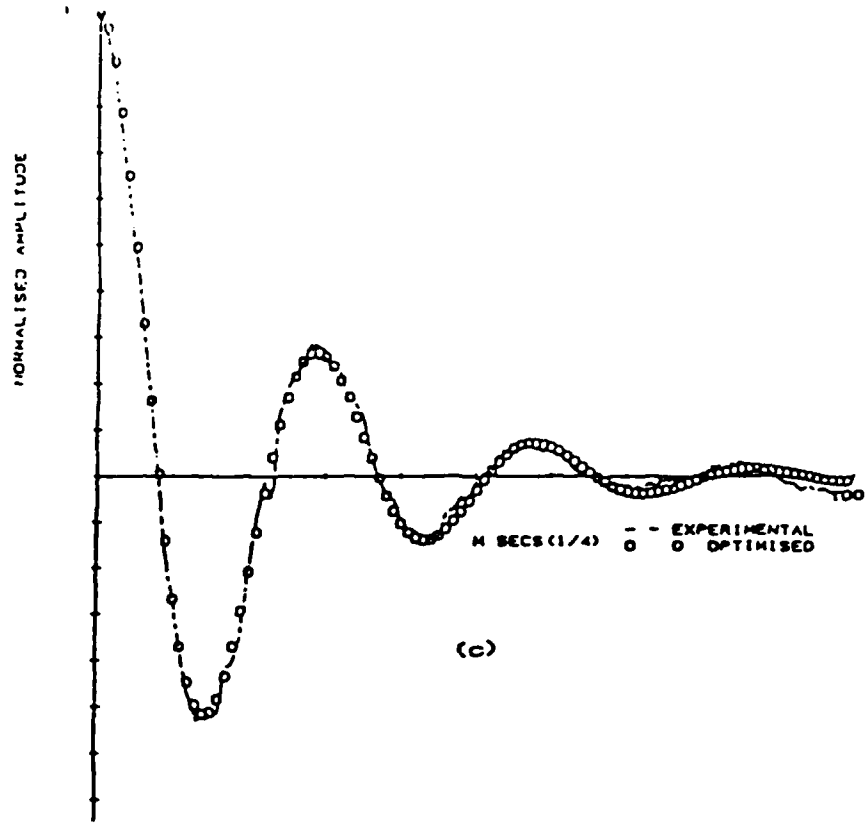
NORMALISED AMPLITUDE
100
M SECS (1/4)
- - EXPERIMENTAL
o o OPTIMISED

(c)

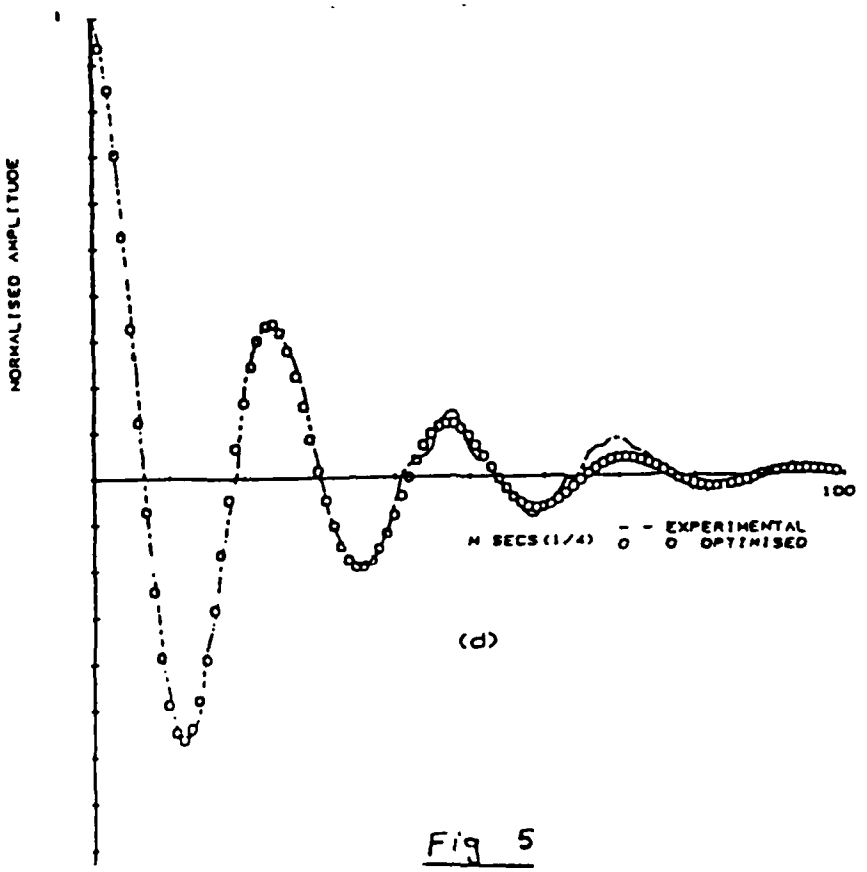
NORMALISED AMPLITUDE
100
M SECS (1/4)
- - EXPERIMENTAL
o o OPTIMISED

(d)

Fig 5

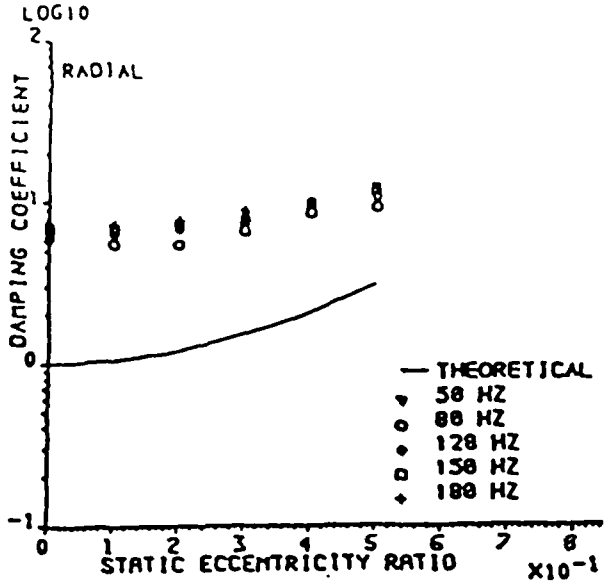
LOG10
RADIAL
DAMPING COEFFICIENT
2
1
0
-1
THEORETICAL
50 HZ
80 HZ
120 HZ
150 HZ
180 HZ
0 1 2 3 4 5 6 7 8
STATIC ECCENTRICITY RATIO
X10-1

(a)

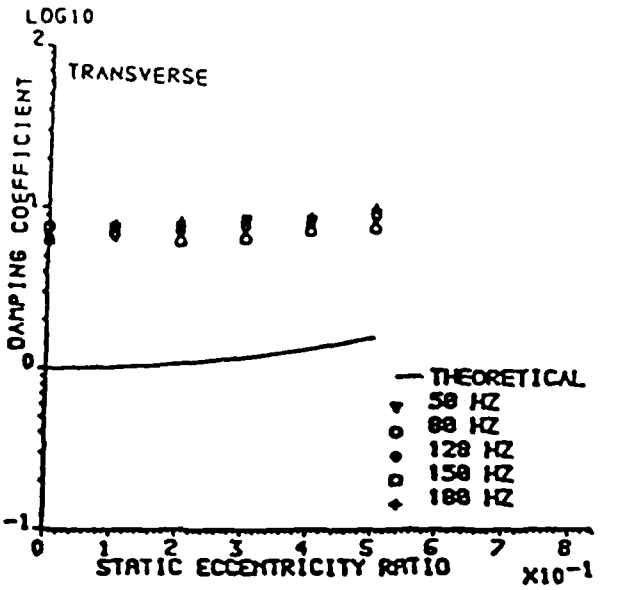
LOG10
TRANSVERSE
DAMPING COEFFICIENT
2
1
0
-1
THEORETICAL
50 HZ
80 HZ
120 HZ
150 HZ
180 HZ
0 1 2 3 4 5 6 7 8
STATIC ECCENTRICITY RATIO
X10-1

(b)

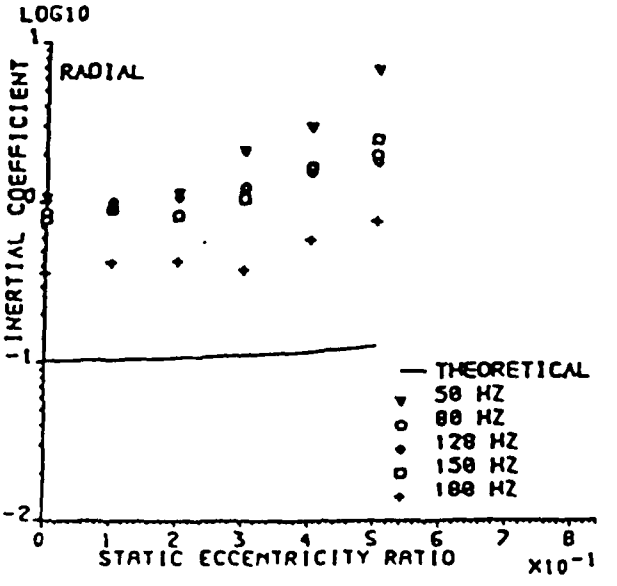
LOG10
RADIAL
INERTIAL COEFFICIENT
1
0
-1
-2
THEORETICAL
50 HZ
80 HZ
120 HZ
150 HZ
180 HZ
0 1 2 3 4 5 6 7 8
STATIC ECCENTRICITY RATIO
X10-1

(c)

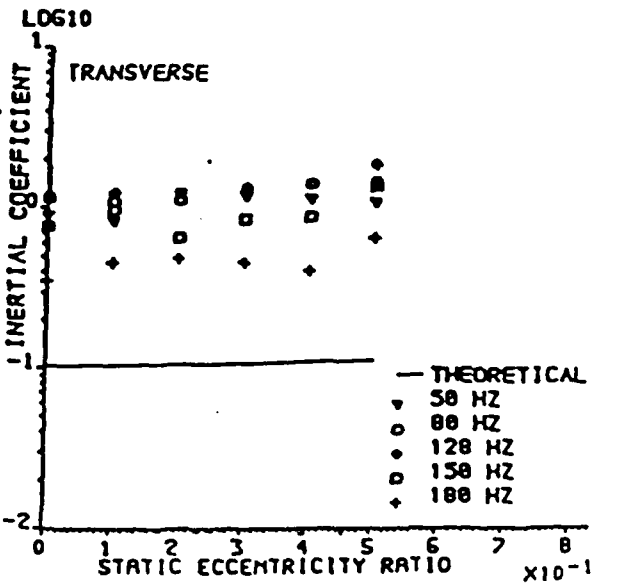
LOG10
TRANSVERSE
INERTIAL COEFFICIENT
1
0
-1
-2
THEORETICAL
50 HZ
80 HZ
120 HZ
150 HZ
180 HZ
0 1 2 3 4 5 6 7 8
STATIC ECCENTRICITY RATIO
X10-1

(d)

Fig. 6

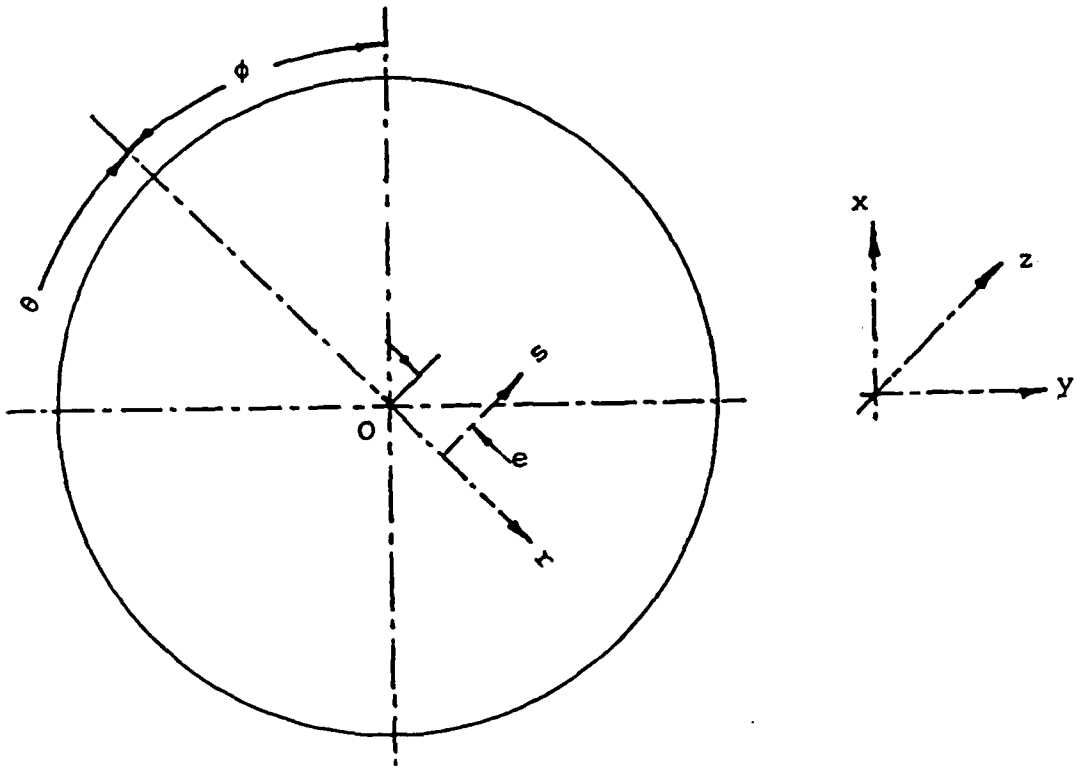

Fig. 1 Bearing diagram

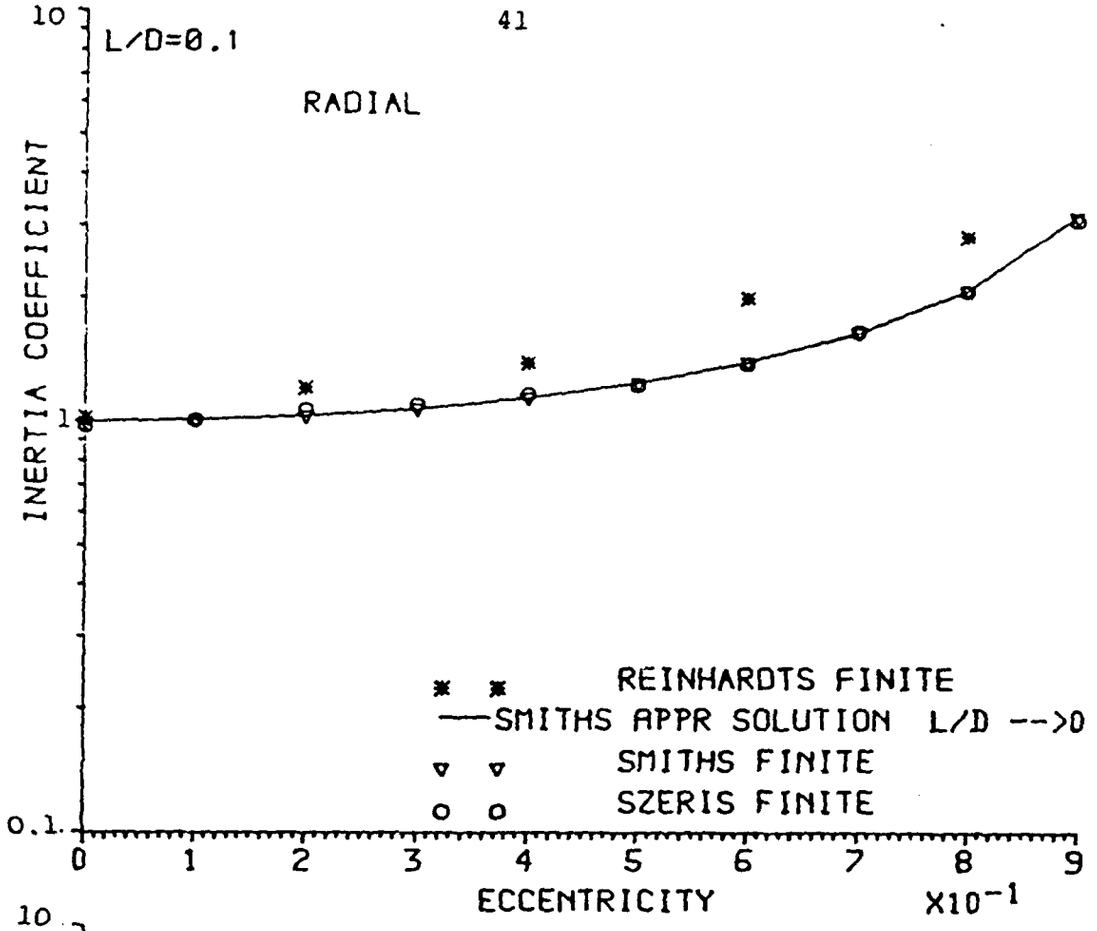
L/D=0.1
RADIAL
INERTIA COEFFICIENT
10
1
0.1
REINHARDTS FINITE
SMITHS APPR SOLUTION L/D -->0
SMITHS FINITE
SZERIS FINITE
0 1 2 3 4 5 6 7 8 9
ECCENTRICITY
X10^-1

(a)

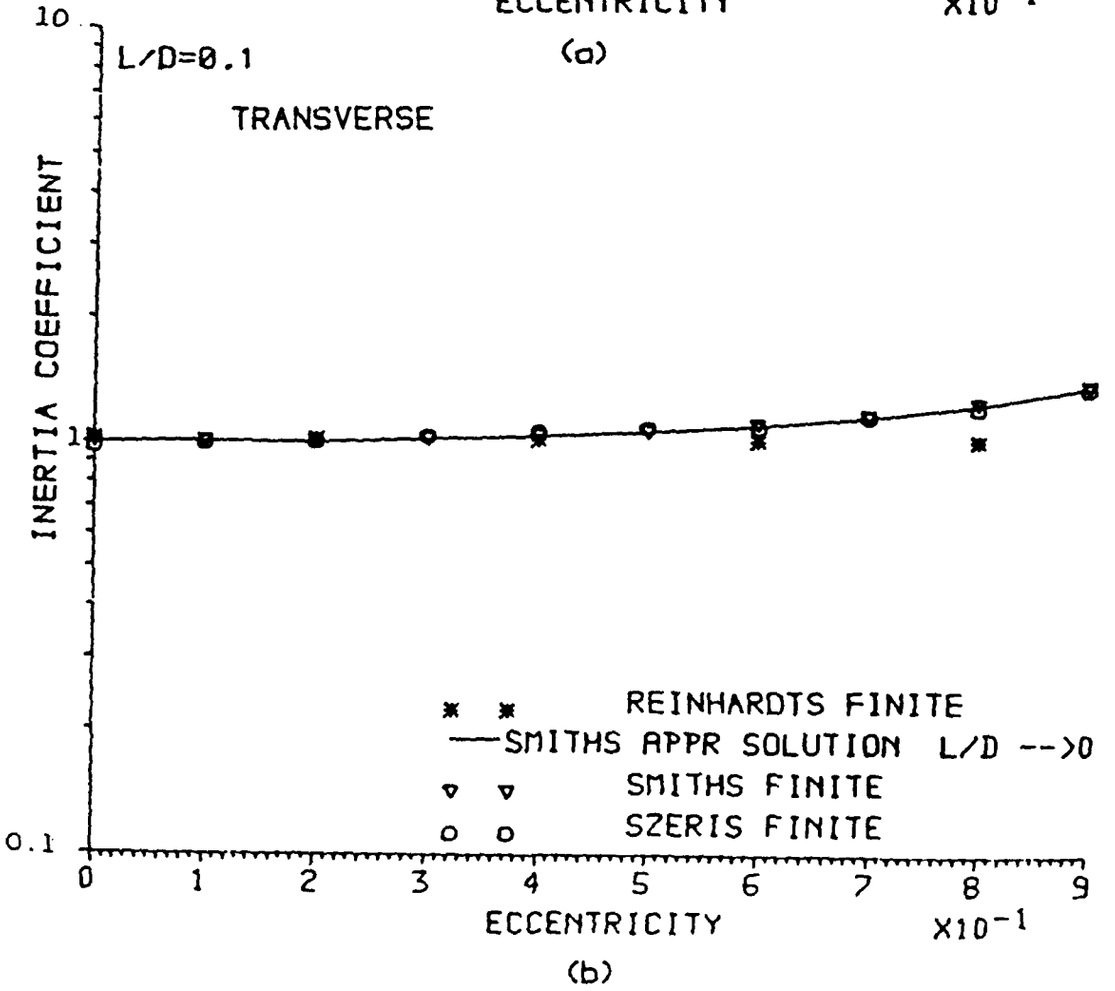
L/D=0.1
TRANSVERSE
INERTIA COEFFICIENT
10
1
0.1
REINHARDTS FINITE
SMITHS APPR SOLUTION L/D -->0
SMITHS FINITE
SZERIS FINITE
0 1 2 3 4 5 6 7 8 9
ECCENTRICITY
X10^-1

(b)

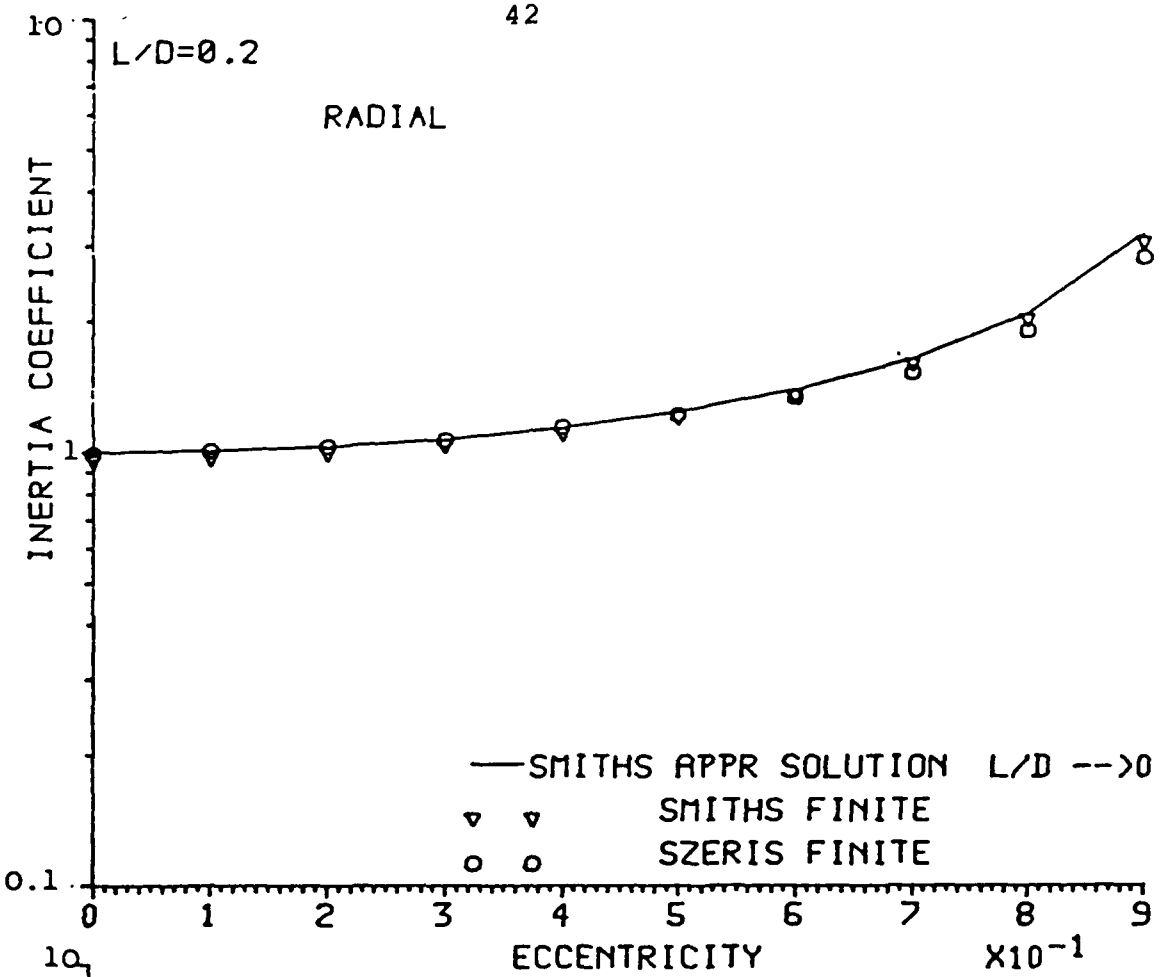
L/D=0.2
RADIAL
INERTIA COEFFICIENT
10
1
0.1
—SMITHS APPR SOLUTION L/D -->0
SMITHS FINITE
SZERIS FINITE
0 1 2 3 4 5 6 7 8 9
ECCENTRICITY X10^{-1}

(a)

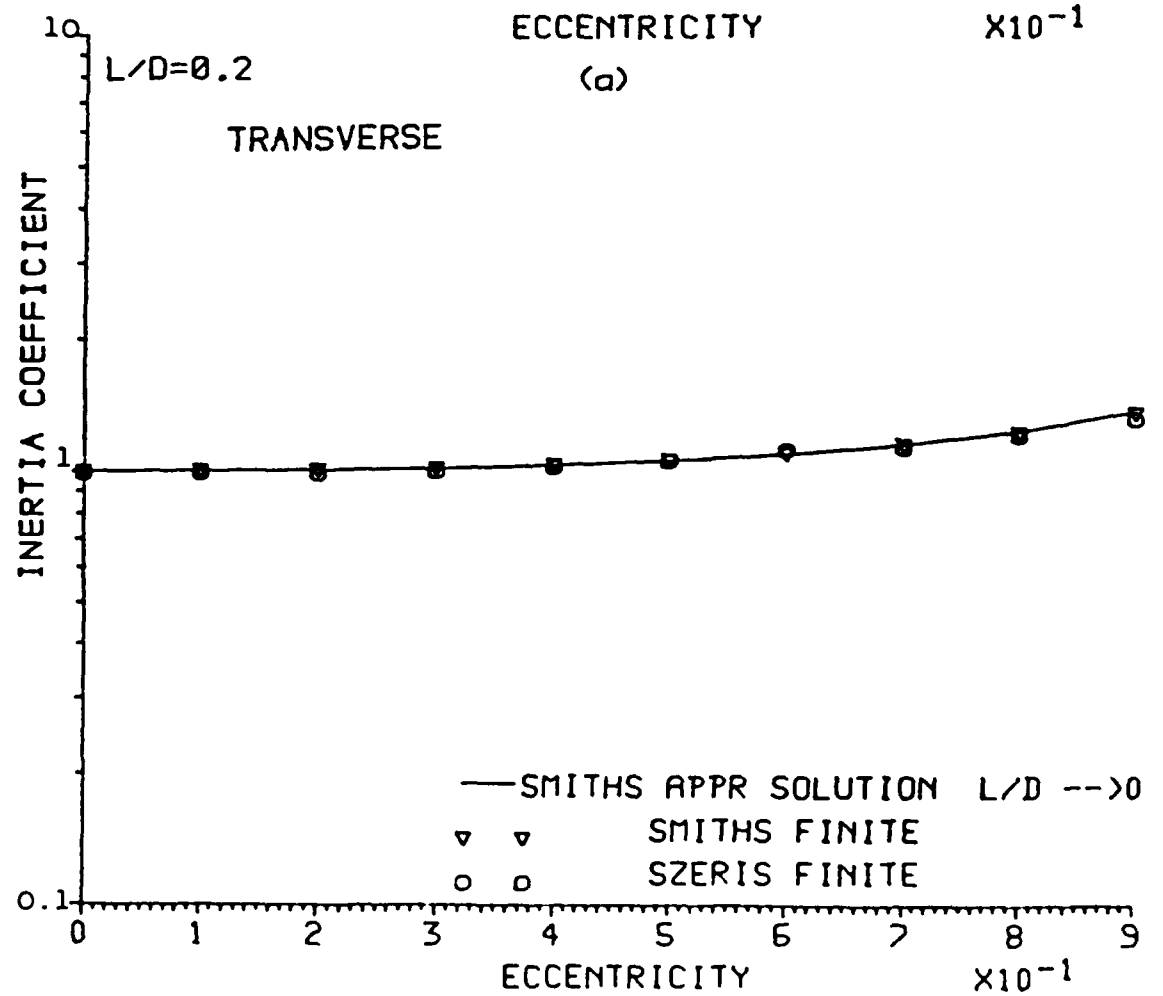
L/D=0.2
TRANSVERSE
INERTIA COEFFICIENT
10
1
0.1
—SMITHS APPR SOLUTION L/D -->0
SMITHS FINITE
SZERIS FINITE
0 1 2 3 4 5 6 7 8 9
ECCENTRICITY X10^{-1}

(b)

Fig. 2

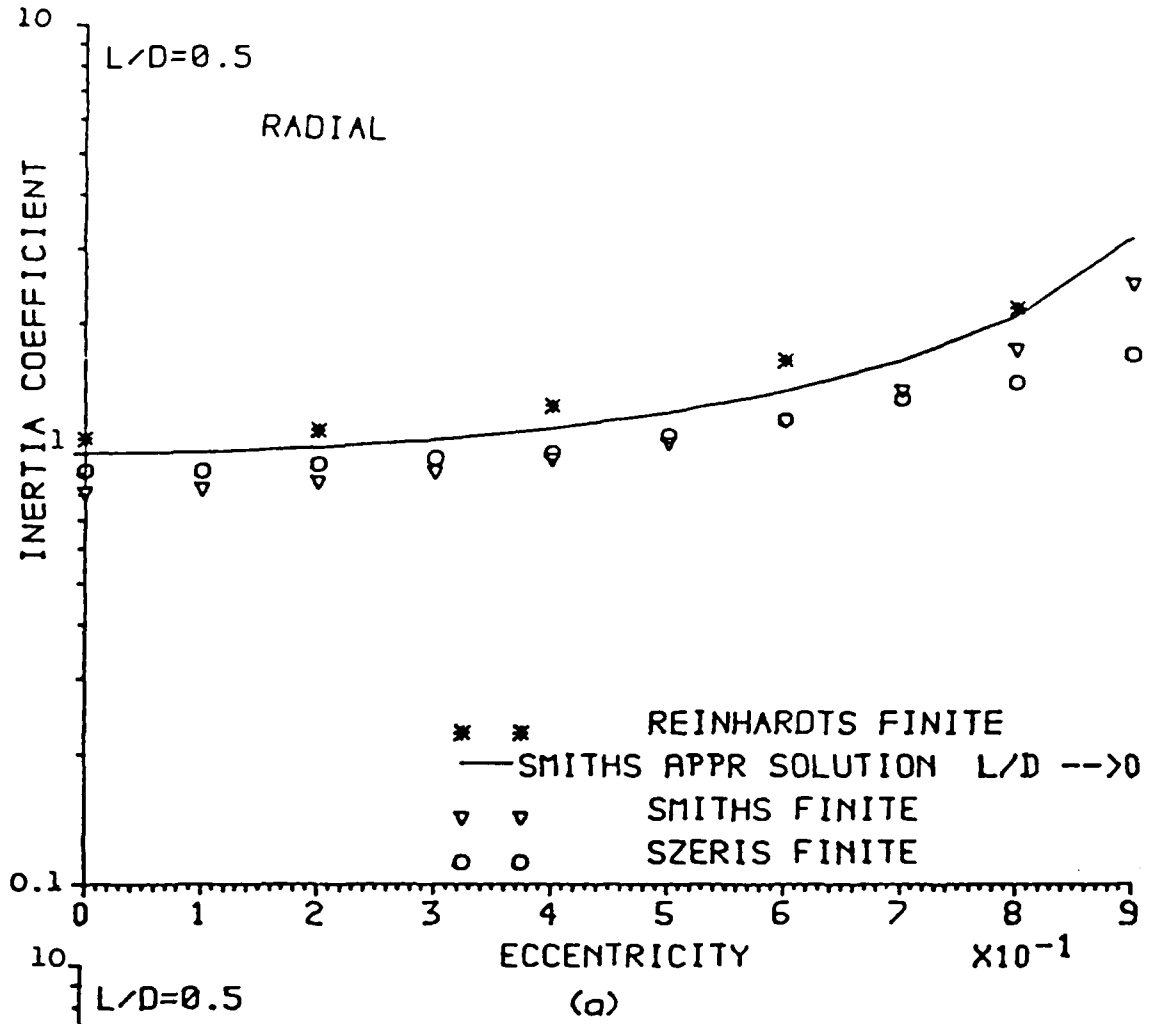
10
L/D=0.5
RADIAL
INERTIA COEFFICIENT
1
0.1
REINHARDTS FINITE
SMITHS APPR SOLUTION L/D -->0
SMITHS FINITE
SZERIS FINITE
0
1
2
3
4
5
6
7
8
9
ECCENTRICITY
X10^-1

(a)

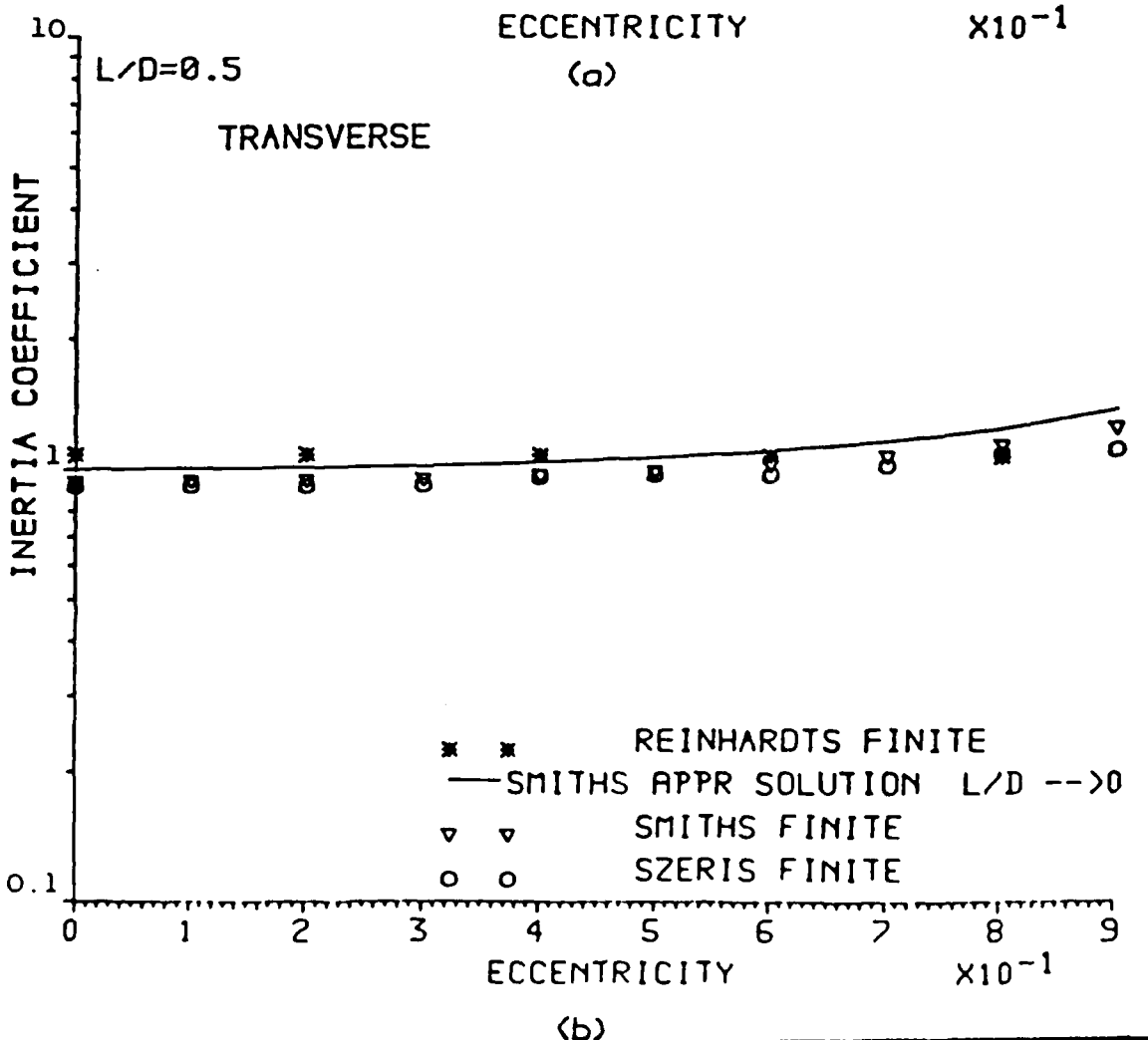
10
L/D=0.5
TRANSVERSE
INERTIA COEFFICIENT
1
0.1
REINHARDTS FINITE
SMITHS APPR SOLUTION L/D -->0
SMITHS FINITE
SZERIS FINITE
0
1
2
3
4
5
6
7
8
9
ECCENTRICITY
X10^-1

(b)

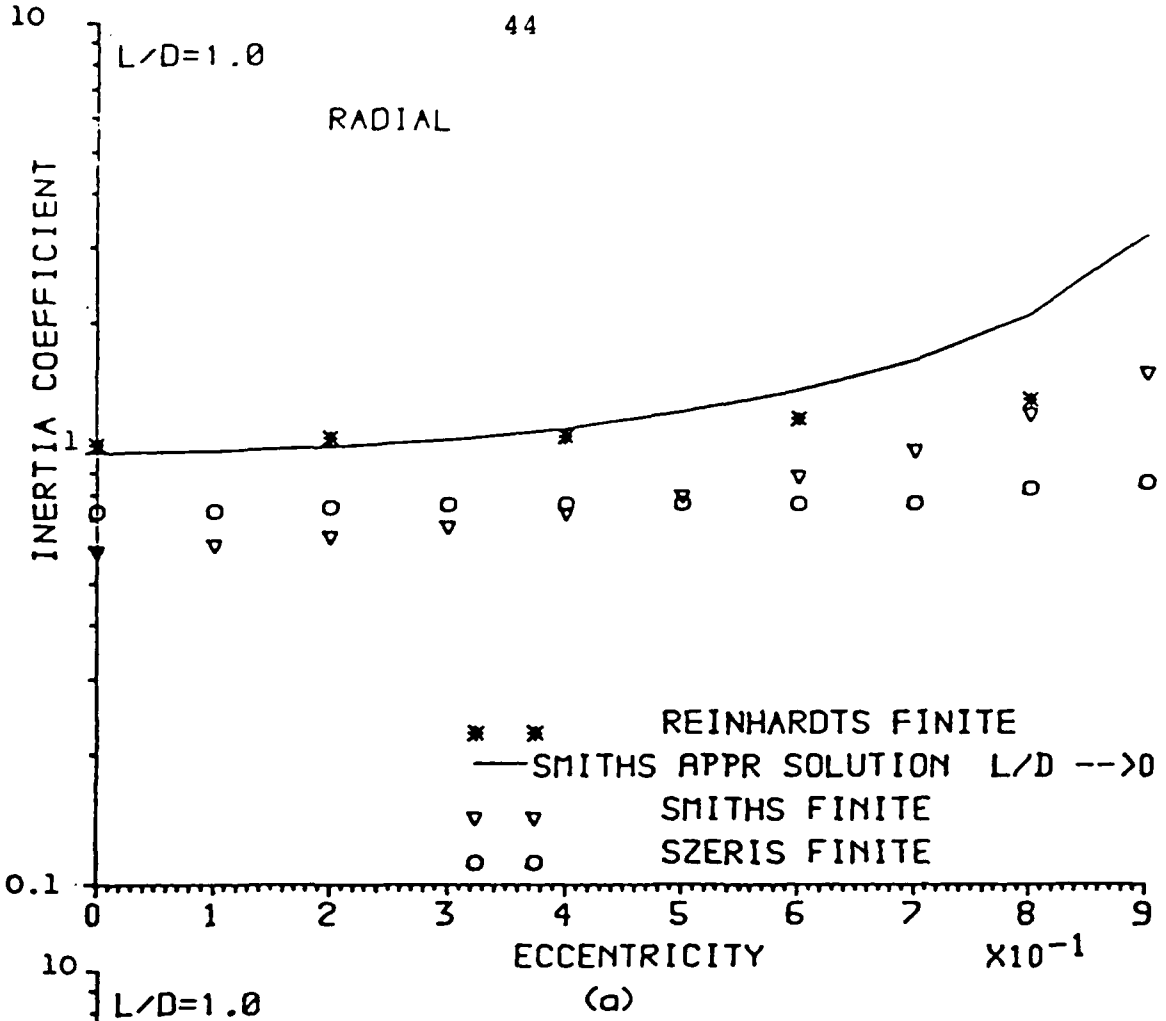
L/D=1.0
RADIAL
INERTIA COEFFICIENT
10
1
0.1
REINHARDTS FINITE
SMITHS APPR SOLUTION L/D -->0
SMITHS FINITE
SZERIS FINITE
0 1 2 3 4 5 6 7 8 9
ECCENTRICITY X10^{-1}

(a)

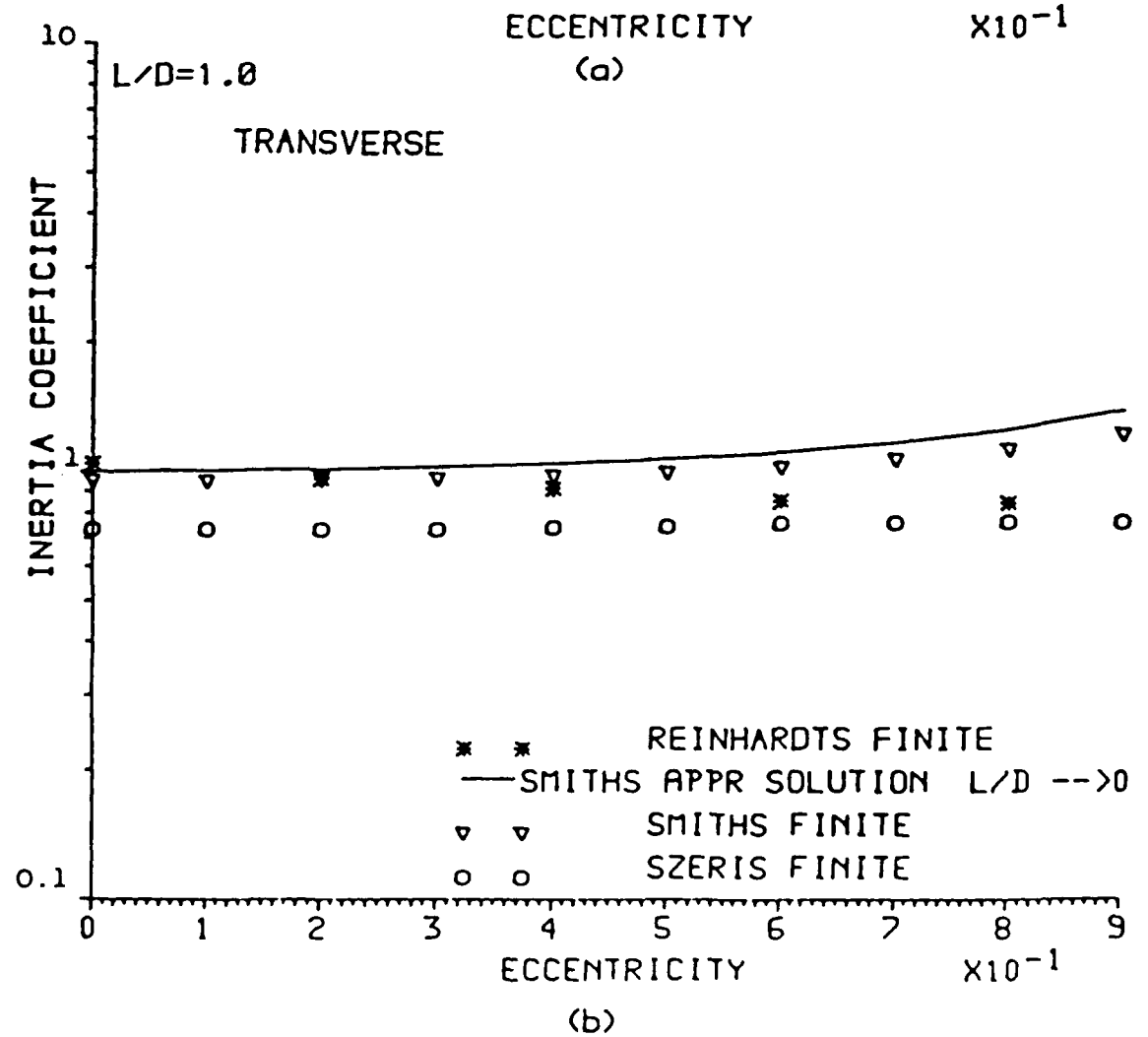
L/D=1.0
TRANSVERSE
INERTIA COEFFICIENT
10
1
0.1
REINHARDTS FINITE
SMITHS APPR SOLUTION L/D -->0
SMITHS FINITE
SZERIS FINITE
0 1 2 3 4 5 6 7 8 9
ECCENTRICITY X10^{-1}

(b)

Fig. 5

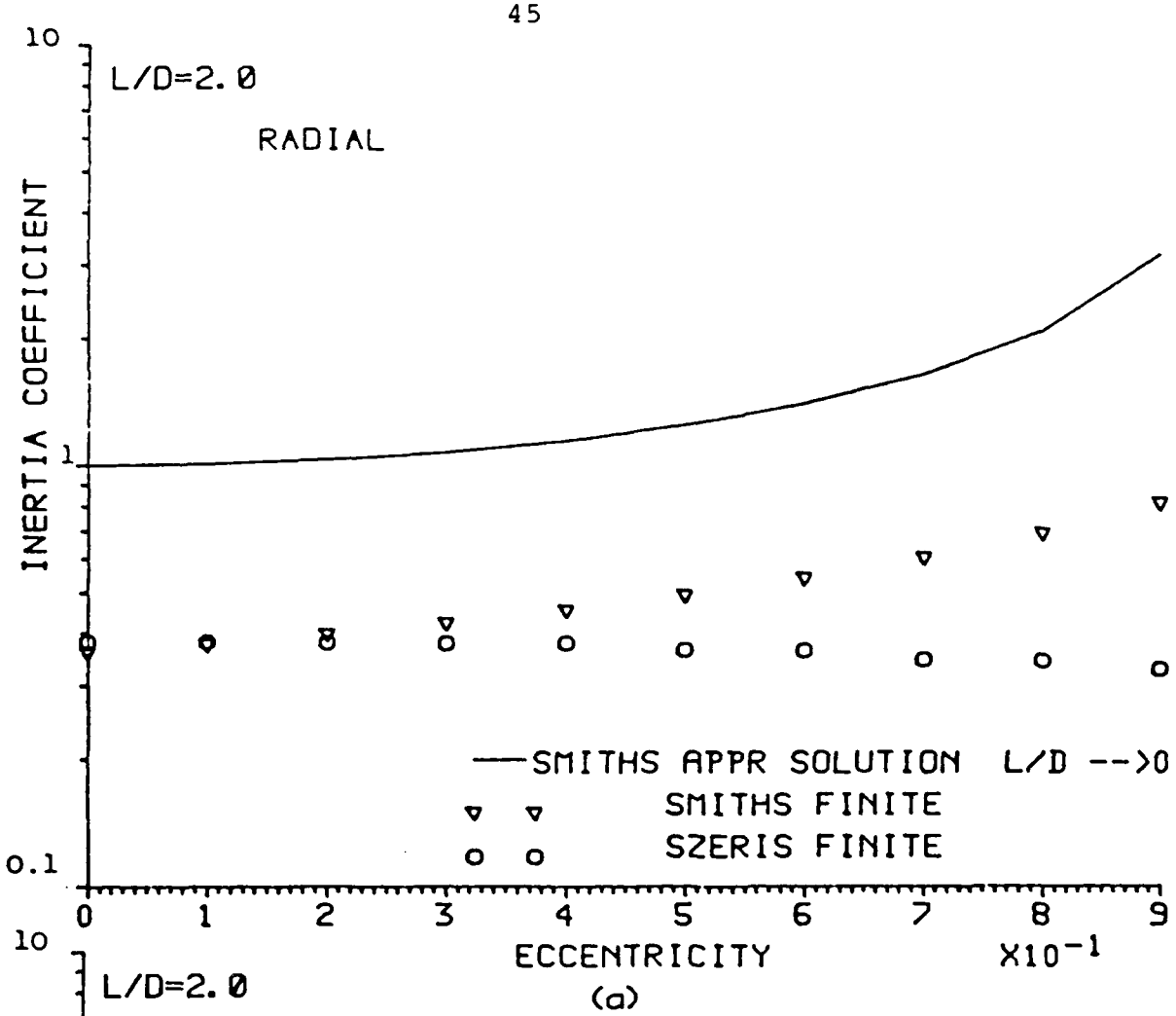
10
L/D=2.0
RADIAL
INERTIA COEFFICIENT
1
0
0.1
—SMITHS APPR SOLUTION L/D -->0
SMITHS FINITE
SZERIS FINITE
0 1 2 3 4 5 6 7 8 9
ECCENTRICITY X10⁻¹

(a)

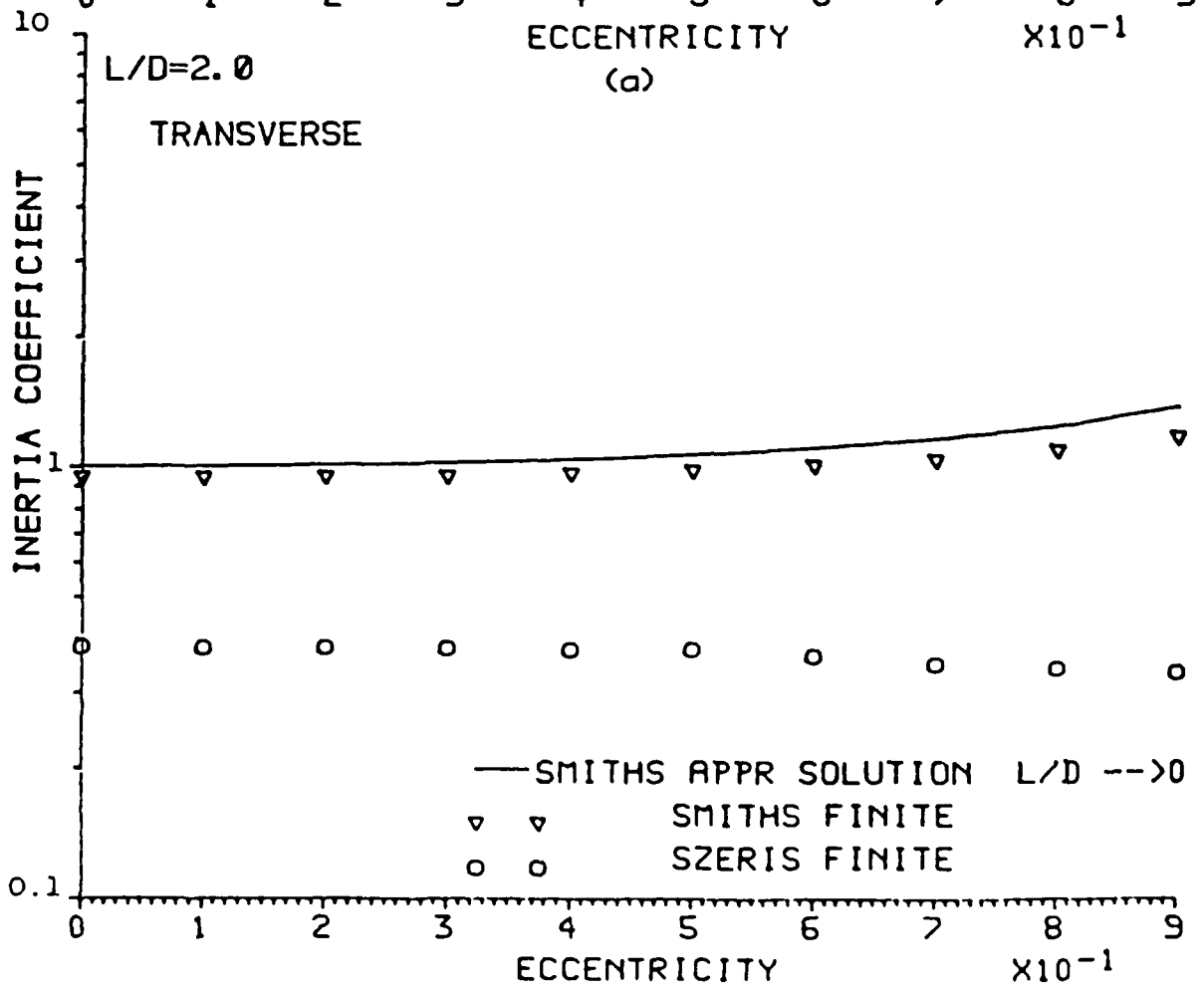
10
L/D=2.0
TRANSVERSE
INERTIA COEFFICIENT
1
0
0.1
—SMITHS APPR SOLUTION L/D -->0
SMITHS FINITE
SZERIS FINITE
0 1 2 3 4 5 6 7 8 9
ECCENTRICITY X10⁻¹

(b)

Fig. 6

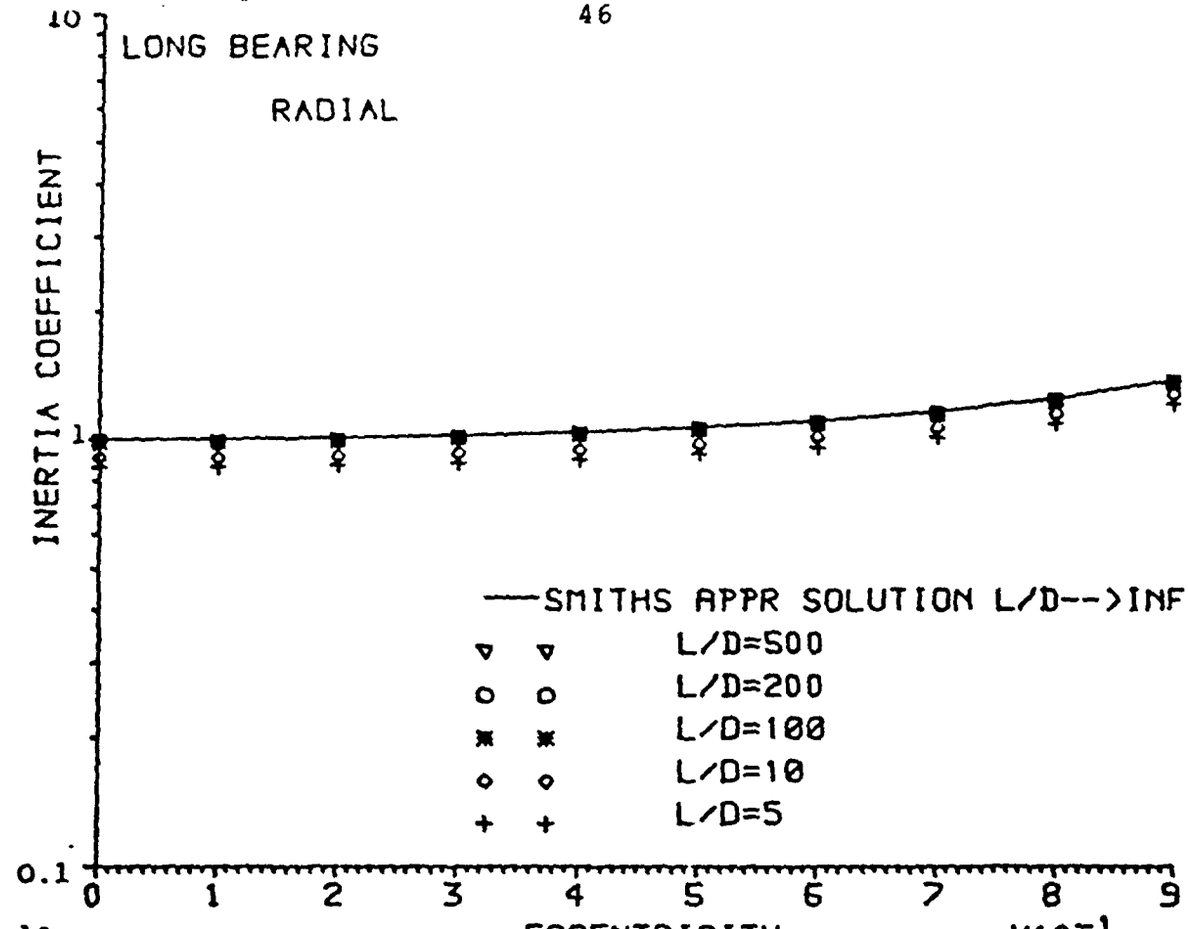
LONG BEARING
RADIAL
INERTIA COEFFICIENT
10
1
0.1
—SMITHS APPR SOLUTION L/D-->INFINITY
L/D=500
L/D=200
L/D=100
L/D=10
L/D=5
0 1 2 3 4 5 6 7 8 9
ECCENTRICITY
X10⁻¹

(a)

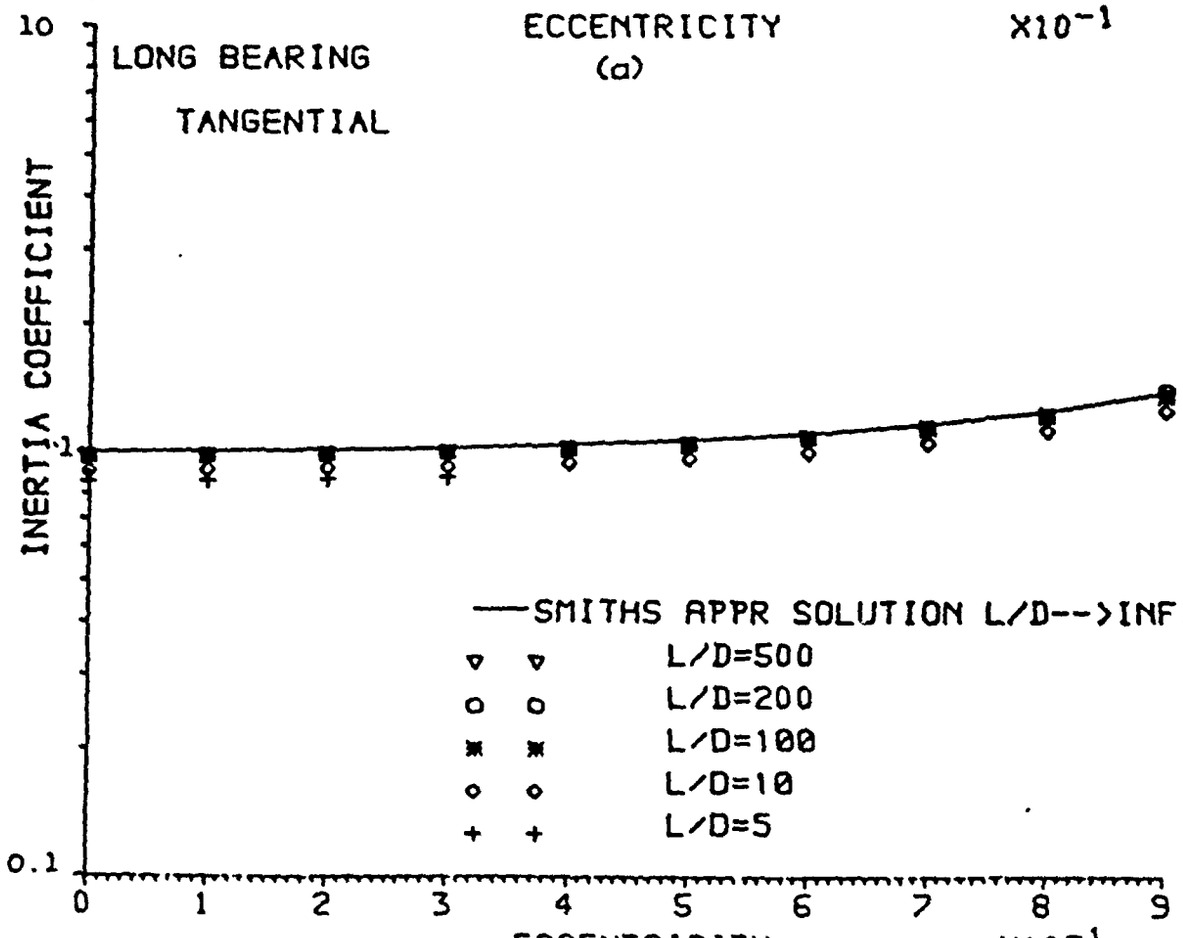
LONG BEARING
TANGENTIAL
INERTIA COEFFICIENT
10
1
0.1
—SMITHS APPR SOLUTION L/D-->INFINITY T
L/D=500
L/D=200
L/D=100
L/D=10
L/D=5
0 1 2 3 4 5 6 7 8 9
ECCENTRICITY
X10⁻¹

(b)

Fig. 7

END

DTIC

8-86